



MINISTRY OF AVIATION

AERONAUTICAL RESEARCH COUNCIL

CURRENT PAPERS

Pressure Distribution
Measurements on a Series
of Slender Delta Body Shapes
at Mach Numbers of 6.85 and 8.60

by

D. H. Peckham

<p>DERA Information Resources</p>		<p>NAME</p> <p>T. B. ...</p>	<p>RETURN BY:</p> <p>17 OCT 2000</p>
		<p>Please return this publication to the Information Centre, or request a renewal by the date last stamped below</p>	
<p>DERA Information Centre No. 1 Building DERA Clapham Bedford MK41 6AE</p>		<p>TEL 01234 225099 FAX 01234 225011 ICE Hurry Pat</p>	

LONDON: HER MAJESTY'S STATIONERY OFFICE

1965

PRICE 6s 6d NET

U.D.C. No. 533.696 : 533.6.048.2 : 533.6.011.55

C.P. No. 791

February 1964

PRESSURE DISTRIBUTION MEASUREMENTS ON A SERIES OF
SLENDER DELTA BODY SHAPES AT MACH NUMBERS OF 6.85 AND 8.60

by

D. H. Peckham

SUMMARY

Results are given of a wind tunnel programme made to study the pressure distributions, mainly on the windward surfaces, of a series of simple body shapes, over a range of angles of incidence up to 29 degrees. It was found that the comparison of experimental pressure distributions with values calculated from various inviscid flow theories and approximations, was complicated by the non-independence of upper and lower surface flow fields, and by boundary-layer-displacement effects. From the few measurements made of upper surface pressure distributions, quite large differences in behaviour were observed between Mach numbers of 6.85 and 8.60. Recommendations are made in regard to future experiments.

CONTENTS

	<u>Page</u>
1 INTRODUCTION	4
2 EXPERIMENTAL DETAILS	4
2.1 Details of models	4
2.2 Details of tests	5
2.3 Experimental accuracy	5
3 DISCUSSION OF RESULTS	6
3.1 Lower surface pressure distributions	6
3.1.1 Models 1, 2 and 3	6
3.1.2 Models 4 and 5	8
3.1.3 Local normal-force characteristics of models 1, 2, 3 and 5	10
3.1.4 Models 6 and 7	11
3.1.5 Models 8 and 9	12
3.2 Upper surface pressure distributions	12
4 CONCLUSIONS AND RECOMMENDATIONS FOR FUTURE WORK	13
REFERENCES	14
ILLUSTRATIONS - Figs.1-18	-
DETACHABLE ABSTRACT CARDS	-

ILLUSTRATIONS

	<u>Fig.</u>
Geometry of models	1
Lower surface pressure distribution for models 1 and 2. M = 6.85	2
Lower surface pressure distribution for models 1 and 2. M = 8.60	3
Lower surface pressure distributions for model 3, M = 8.60	4
Mach number to give attached plane shock wave on wings 4 and 5	5
Variation of shock stand-off angle with incidence on wings 4 and 5	6

ILLUSTRATIONS (CONTD)

	<u>Fig.</u>
Lower surface pressure distributions for wings 4 and 5. M = 6.85	7
Effect of positive sideslip on lower surface pressures on wing 5. M = 6.85	8
Variation with incidence of mean pressure coefficient on lower surfaces of wings 1, 2 and 5. M = 6.85	9
Variation with incidence of mean pressure coefficient on lower surfaces of wings 1, 2 and 3. M = 8.60	10
Effect of viscous interaction on lift/drag ratio obtained from lower surfaces of wings 1 and 2	11
Pressure distributions over the lower surfaces of wings 6 and 7 at M = 6.85 and 8.60	12
Geometry of shock wave on model 7. M = 6.85	13
Lower ridge-line pressures on wings 6 and 7	14
Variation with local incidence of mean pressure coefficient on lower surfaces of wings 1, 2 and 7. M = 6.85	15
Variation with local incidence of mean pressure coefficient on lower surfaces of wings 1, 2 and 7. M = 8.60	16
Lower surface pressure distributions for models 8 and 9, including effect of interference from delta wings. M = 8.60	17
Upper surface pressure distributions for model 1. M = 6.85 and 8.60	18

1 INTRODUCTION

For hypersonic Mach numbers, while exact methods exist for designing some types of lifting body shapes to support specified inviscid flow fields, no exact methods exist for calculating pressure distributions on lifting body shapes in general. Two aspects of this problem which can be investigated in wind tunnels are:-

(i) With bodies designed for specified inviscid flow fields, to find out how such bodies behave when viscous effects are present; also, it is just as important to investigate how they behave under conditions of off-design Mach number and incidence, and at yaw.

(ii) Since it may not always be possible to solve a design problem by designing a body shape for a specified flow field - e.g. if large ranges of incidence and Mach number need to be covered, to obtain information of a more general nature on the behaviour of a variety of lifting body shapes.

A programme of work on the above lines is under way in the R.A.E. intermittent hypersonic tunnel^{1,2,3}.

This paper gives the results of pressure-plotting experiments on a series of eight conical models (and one two-dimensional model), at Mach numbers of 6.85 and 8.60 and angles of incidence up to 29 degrees. Pressure-plotting experiments were chosen, rather than overall force measurements, since it was considered that such an approach would give a better understanding of the flow. Even so, it is recognised that more detailed tests will eventually be necessary. For example, pressure measurements on their own were not always sufficiently revealing, and measurements of shock wave shape, and local velocity distributions and directions are needed in addition; also, when boundary layer effects arise, a knowledge of surface temperature distribution is important.

The experimental results are compared with values calculated from three often-used empirical methods for predicting pressures, the tangent-wedge, tangent-cone and Newtonian approximations³. In the case of the bodies designed to support plane shocks², i.e. where a two-dimensional flow field is specified, the tangent-wedge approximation becomes, in fact, an exact inviscid theory. Otherwise, these methods do no more than show what pressure distributions would result if certain simple flow fields were obtained. That these simple flow fields are rarely obtained is shown by the measured pressure distributions; nevertheless, these methods are of some value for comparison purposes.

2 EXPERIMENTAL DETAILS

2.1 Details of models

Six models were used, but since three of these were each tested in two different orientations, effectively nine different body shapes were available. So for convenience each of these has been allotted its own model number, and they have been numbered in the order in which the experimental results are discussed in Section 3. Geometric details of these models are given in Fig.1, with the position of the reference axis for model incidence marked.

With the exception of model 4, all were conical, their shapes being related to a circular cone of unit aspect ratio (model 9). Thus one shape was a half-cone tested both ways up (models 1 and 8), another shape a half-pyramid tested both ways up (models 2 and 7), and another a pyramid tested in two attitudes (models 3 and 6). Model 5 was a variant of model 1, having an inverted-V cut-out on its lower surface, and model 4 was a two-dimensional version of model 5; these two models (4 and 5) were designed to support plane attached shock waves at certain combinations of angle of incidence and Mach number².

On all the conical models, pressures were measured across the semi-span on both upper and lower surfaces at a station two-thirds of the root chord from the model apex; on model 4, pressures were measured on the lower surface only. A small number of pressure holes were also included on the opposite semi-span of the models, and at a station one-third of the root chord from the model apex, to check for symmetry and to see whether the flow was conical.

2.2 Details of tests

The tests were made in the 7 in. x 7 in. intermittent hypersonic tunnel at R.A.E. Farnborough, at Mach numbers of 6.85 and 8.60, with a stagnation pressure of 750 p.s.i.g., and stagnation temperatures of approximately 650°K and 800°K, respectively. In order to cover an incidence range up to 29 degrees while keeping the models in the central core of uniform flow in the working section, it was necessary to restrict model lengths to 5 inches, so the Reynolds numbers based on model lengths were about 2.5 million and 0.9 million, for the Mach numbers of 6.85 and 8.60, respectively. Pressures were measured on a conventional multi-tube mercury manometer bank, with one or more tubes connected to a vacuum reference. Steady readings were obtained after some 45-60 seconds running, when the manometer was clamped and the tunnel shut down. (This long settling time was mainly due to the use of 1 mm O.D. hypodermic pressure tubing; more recent experience has shown that this settling time can be reduced to about 15 seconds by using $\frac{1}{2}$ mm O.D. tubing instead.)

2.3 Experimental accuracy

Evidence suggests that manometer readings were measured to an accuracy of better than ± 0.02 in. This error, combined with a similar error in reading the reference pressure, would result in a maximum error of ± 0.003 in pressure coefficient, C_p , at $M = 6.85$ and ± 0.008 in C_p at $M = 8.60$. Errors in setting the angles of incidence of the models could amount to a further error in C_p of up to ± 0.002 . The possible maximum direct measuring error was therefore ± 0.005 in C_p at $M = 6.85$ and ± 0.010 at $M = 8.60$. As well as a measuring error, there were errors arising from lack of flow uniformity in the test section, the variation of dynamic pressure in the region of the model being about $\pm 1\%$ of the mean value.

On the basis of the above figures, the estimated maximum experimental errors, and R.M.S. experimental errors, are tabulated below:-

C_p	<u>Maximum error in C_p</u>		<u>R.M.S. error in C_p</u>	
	M = 6.85	M = 8.60	M = 6.85	M = 8.60
0.1	±0.006	±0.011	±0.004	±0.008
0.3	±0.008	±0.013	±0.005	±0.009
0.5	±0.010	±0.015	±0.006	±0.010

The extent of these estimated maximum experimental errors is marked by an 'I' on the Figures in which measured pressure distributions are plotted. The R.M.S. errors are approximately two-thirds of the maximum errors.

The greatest proportion of the errors given in the above table arises from the inaccuracy of pressure measurement, particularly for low values of C_p at the higher Mach number. In future tests, this error will be largely eliminated by the use of oil rather than mercury manometers, with the result that the errors listed above will be approximately halved.

A check on experimental accuracy comes from a comparison of pressures measured at the 1/3-root chord station, and the 2/3-root chord station. This comparison showed that the flow was symmetrical, and apparently conical, within the error limits given above. However, as will be seen later in Section 3, there is evidence of the presence of boundary layer self-induced pressures of the same order as the experimental error. If this was so, the variation of boundary layer displacement thickness with length would cause a pressure gradient, and the flow would not be conical. This difficulty will only be resolved when more accurate measurements are made.

3 DISCUSSION OF RESULTS

3.1 Lower surface pressure distributions

3.1.1 Models 1, 2 and 3

These models all had flat lower surfaces. Pressure distributions on models 1 and 2 at Mach numbers of 6.85 and 8.60, are plotted in Figs.2 and 3, respectively; also plotted are estimates of the pressure distributions obtained from three well-known empirical methods³, the tangent-wedge, tangent-cone and Newtonian approximations. All these give constant pressures across the span.

From examination of Figs.2 and 3, the following observations can be made:-

(i) The results for a Mach number of 6.85 show little or no difference between the pressure distributions for the two body shapes, the differences that are present being within the estimated limits of experimental error; for a Mach number of 8.60 the pressure distributions at incidences of 18 and 24 degrees differ by up to 10%, but even so this difference is just within

the possible limits of experimental error. However, a consistent tendency at the larger angles of incidence for the pressures on model 2 to be slightly higher than those on model 1, particularly near the leading edges, cannot definitely be dismissed as experimental error. This difference, if real, would have to be caused by some sort of interaction between the flows over the upper and lower surfaces of the models - even though the components of Mach number normal to their leading edges were supersonic (for $M = 6.85$, $\beta s/\ell = 1.7$; for $M = 8.60$, $\beta s/\ell = 2.14$). That such an interaction could be present was revealed by shadow pictures (in plan view) which showed that detached shocks were obtained, i.e. the leading edges were in a conically subsonic region. Further evidence that the upper and lower surface flows were not independent comes from the fact that at zero incidence, where one might expect the lower surface to be at free stream pressure, a positive pressure was in fact measured. A similar effect has been reported in Ref.4 (but see (ii) below).

(ii) However, different pressure coefficients were obtained at zero incidence for the two test Mach numbers; so these positive pressure coefficients are probably not due solely to the non-independence of the upper and lower surface flows, but also to a boundary layer displacement effect. The excess pressure coefficient* induced in this way by a two-dimensional laminar boundary layer on a flat plate at zero incidence, has been shown⁵ to be proportional to M/R_x^2 , where R_x is the local Reynolds number at the pressure hole position. For the present tests this means that the excess pressure coefficient would be twice as great at $M = 8.60$ as at $M = 6.85$. Such an effect is probably the explanation why higher mean pressure coefficients were obtained for the lower angles of incidence at $M = 8.60$ than at $M = 6.85$.

Clearly, there is a need for further experimental work before the effects described in (i) and (ii) above can be separated and more accurately defined.

(iii) In regard to the pressure distributions obtained at the higher angles of incidence, it was found that they were not uniform, but that pressures tended to increase towards the leading edges. From this fact, it can be inferred that the shocks were not plane, as is assumed by the tangent-wedge approximation. For $\alpha = 6^\circ$, the pressure coefficients measured at

*It is more usual to give boundary-layer-induced pressures in terms of the free stream static pressure, p_∞ , and the viscous interaction parameter

$$\chi = M^3/R_x^2,$$

i.e.
$$\frac{p - p_\infty}{p_\infty} = k_1 \left(k_2 + k_3 \frac{T_w}{T_s} \right) \chi,$$

where k_1 , k_2 and k_3 are constants, and T_w/T_s the ratio of wall temperature to stagnation temperature. In the present Note, for consistency, all results are

given in pressure coefficient form, i.e.
$$C_p = \frac{p - p_\infty}{\frac{\gamma}{2} p_\infty M^2}.$$

$M = 8.60$ were higher than those at $M = 6.85$, but for $\alpha = 12^\circ$ and above, the reverse was the case, as would be expected from an inviscid point of view (judging from the exact inviscid solutions for wedges and cones). It would appear, therefore, that the viscous effects described in (ii) above, decrease in magnitude with increase of incidence, and become relatively unimportant for incidences of 12 degrees and more. This is in agreement with an analysis by Hayes and Probst⁶, who have shown that the boundary-layer-induced pressure on an inclined flat plate is smaller than the induced pressure on a flat plate at zero incidence, by a factor $1/(Ma)^2$, when $(Ma)^2 \gg 1$.

Pressure distributions on model 3 at a Mach number of 8.60 are given in Fig.4. This model was of aspect ratio 0.707, as compared with unity for models 1 and 2. For model 3, the incidence, α , was measured relative to its centre line, so a new symbol θ is therefore introduced, where θ is the local incidence of the lower flat surface, so that the pressure distributions on models 1, 2 and 3 can be compared on a common basis. Thus for models 1 and 2 $\theta = \alpha$, and for model 3, $\theta = \alpha + 10^\circ$. With model 3, the mean pressure coefficient was slightly above the tangent-wedge value for a local incidence of 10 degrees, but fell progressively below this value with increase of incidence. This behaviour is broadly the same as was obtained with models 1 and 2, except that the pressure distributions on model 3 were more uniform at the higher angles of incidence than was the case with models 1 and 2. Unfortunately, a direct comparison of pressure distributions on model 3 with those on models 1 and 2 is not possible, since the tests were made at different local angles of incidence. Instead, the variation of the mean pressure coefficients on these models with local incidence have been compared (see Section 3.1.3 and Fig.10).

3.1.2 Models 4 and 5

The geometry of models 4 and 5 was chosen so that at the test Mach number of 6.85 a plane shock wave should be obtained at two convenient angles of incidence², and also so that over a fairly wide incidence range the Mach number for shock attachment should not be far removed from $M = 6.85$. Thus from Fig.5 it can be seen that for $7^\circ < \alpha < 15^\circ$, the "design" Mach number varies only within the limits 6.85 ± 0.10 . In fact, shadow photographs showed that the plane attached shock wave condition was not achieved, the shock wave never approaching closer than $\frac{1}{2}$ degree to the plane of the leading edges (Fig.6). There was no apparent difference in shock wave angle between models 4 and 5. This is possibly due to the displacement effect of the boundary layer. A calculation by the method of Catherall¹⁶ of the boundary layer displacement thickness at the rear of the model, gave a displacement thickness of 0.036 in. on the model centre line, which is roughly equivalent to a deflection of the external flow by about $1/3$ degrees. However, these shadow pictures showed only the most windward extremity of the shocks, so it could have been that the shocks were attached, or nearly attached, but bowed outwards away from the wing surfaces.

The pressure distributions measured on models 4 and 5 are plotted in Fig.7. For both models, throughout the incidence range covered, the pressures obtained were greater than would be achieved from a two-dimensional deflection of the flow through an angle equal to the angle of incidence (i.e. the tangent-wedge assumption). This is consistent with the shock waves

being at a greater incidence than expected, as was observed in the shadow photographs, since a greater shock angle than the design angle implies a higher pressure behind the shock than the design value. So alternatively, if it is assumed that the shocks shown by the shadowgraph pictures were plane, the pressures which would be obtained on plane surfaces behind such shocks can be calculated from the formula²:-

$$C_p = \frac{5}{3} (\sin^2 \zeta - 1/M^2) \quad (1)$$

where ζ is the measured incidence of the shock to the free stream.

Pressure coefficients calculated from this expression are shown in Fig.7. For angles of incidence of 5.4, 7.4 and 9.4 degrees it can be seen that the measured pressures, for both models, fall between values calculated from the tangent-wedge method and equation (1). This result presumably means that the shadow pictures for these angles of incidence were not showing detached plane shocks, but shocks bowed outwards from the wing surfaces. On the other hand, for angles of incidence of 11.4 degrees and greater, the mean pressure distributions were nearer to values given by equation (1); so for these incidences it is possible that the shocks were approximately plane, and detached.

The effect of 5 degrees sideslip on the pressure distribution on model 5 is illustrated in Fig.8, for the two angles of incidence (7.4 and 13.4 degrees) at which an attached plane shock wave should be obtained at $M = 6.85$, and also for an incidence (19.4 degrees) well above the design condition. Shadow pictures showed no apparent change in shock angle from the zero sideslip condition, but did show some "thickening" of the shock, which can presumably be interpreted as a distortion of the shock shape from its symmetrical shape at zero sideslip. For the wing at the design angles of incidence, sideslip caused little change in pressure over the middle third of the lower surface, a decrease in pressure on the leading wing-half and an increase on the trailing wing-half, these changes being greatest near the leading edges. Thus positive sideslip gives a positive rolling moment, which is the conventional anhedral effect. Similar results have been obtained by Treadgold⁷ at supersonic Mach numbers. The behaviour of such wings at design and off-design incidence and Mach number, and with sideslip, is the subject of a report in preparation.

Estimates have been made by Bagley⁸ of the lateral forces and moments on these wing shapes when yawed, on the assumption that the yawed wing supports two plane attached shocks which do not mutually interfere. It was found that this simplified flow pattern was only possible for small yaw angles, of around one degree or less, so this method is not really applicable to the 5 degrees yaw of the present tests. Even so, an estimate by this method is shown in Fig.8 on the assumption that Bagley's results can be linearly extrapolated to 5 degrees yaw. This shows a gross overestimate of the rolling moment, and clearly the Bagley flow model is not adequate for such large yaw angles.

3.1.3 Local normal-force characteristics of models 1, 2, 3 and 5

It is convenient to compare the normal-force characteristics of these wings at this stage. The lower-surface pressure distributions given in Figs. 2, 3, 4 and 7 have been integrated to give local normal-force coefficients, and these are plotted in Figs. 9 and 10, for Mach numbers of 6.85 and 8.60 respectively.

Putting aside for the moment the complications arising at low angles of incidence from the non-independence of the flows over the upper and lower surfaces, and from boundary-layer-displacement effects, we find that although the pressure distributions on wings 1 and 2 were not uniform, that for incidences up to about 15 degrees the mean pressure coefficients for these wings are the same as for an infinite flat plate (i.e. tangent-wedge value), to an accuracy sufficient for most practical purposes (Fig. 9). This result is in agreement with a recent theoretical study by Babaev⁹, who has demonstrated that, for the lower angles of incidence, the mean pressure coefficient on flat delta wings with attached shocks differs by only a few per cent from that which would be obtained on an infinite flat plate, at the same conditions of Mach number and incidence. As discussed in the previous section, the pressures (and therefore the normal forces) measured on wing 5 were greater than the values appropriate to an infinite flat plate, since the designed attached shock condition was not achieved.

If we now look at the results for $M = 8.60$ in Fig. 10, we see that for the low angles of incidence it is impossible to judge the validity of inviscid theories from the limited information which is available. This leads one to the conclusion that pressure-plotting experiments on their own are not always sufficient; in this case, clearly one needs to know also the shock shape, in order to check the basic assumptions of any inviscid theory, and details of the boundary layer in order to estimate its displacement effect. In fact, it has been concluded by Goebel et al¹⁰ from correlations of wind tunnel data in the range $0.1 < \chi_L < 1.1$, that when calculating lift/drag ratios, boundary-layer-displacement corrections to surface pressure and skin friction are required whenever χ_L is greater than 0.2 ($\chi_L = M^3/R_L^{\frac{1}{2}}$, where L is the root chord length of a delta wing). In the present tests, the values of χ_L were 0.2 at $M = 6.85$ and 0.65 at $M = 8.60$.

An illustration of the boundary-layer-displacement effect on the lift/drag ratios obtained from the lower surfaces of wings 1 and 2 is given in Fig. 11. The experimental results are compared in the first instance with inviscid two-dimensional theory, but since this gives the artificial result of $L/D \rightarrow \infty$ as $C_L \rightarrow 0$, a second set of curves is given where an allowance has been made for a contribution to drag from skin friction, a value of $C_f = 0.003$ being used in all cases for simplicity. For $M = 6.85$ and $\chi_L = 0.2$, the boundary-layer-displacement effect on L/D ratio is small, only a few per cent for $0.05 < C_L < 0.10$, but the effect is much larger, i.e. some 40% on L/D ratio at $C_L = 0.05$, for a value of $\chi_L = 0.65$. Of course, there will be an

opposite, but generally not equal, effect on L/D ratio arising from the viscous interaction on the upper surface, so that the overall effect on L/D ratio would not in practice be as large as that shown in Fig.11. (It is worth pointing out here that the full scale value of χ_L is almost certainly less than 0.1 for low hypersonic Mach numbers.)

3.1.4 Models 6 and 7

The pressure distributions measured on these models at Mach numbers of 6.85 and 8.60 are plotted in Fig.12. For these shapes, the local incidence, θ , is constant over each facet, and its value can be obtained from an expression derived in Ref.11:-

$$\sin \theta = \frac{\cos \alpha + \sin \alpha \cot \varepsilon}{(1 + \cot^2 \delta + \cot^2 \varepsilon)^{\frac{1}{2}}} \quad (2)$$

where ε = semi-thickness angle in the plane of symmetry

$$\delta = 90^\circ - (\text{leading-edge sweep}).$$

For models 6 and 7, $\cot \delta = \cot \varepsilon = 4$, and equation (2) reduces to $\sin \theta = (\cos \alpha + 4 \sin \alpha)/33^{\frac{1}{2}}$.

From examination of Fig.12, the following observations can be made:-

(i) Although the small differences in pressure distribution between models 6 and 7 could be due to experimental error, at the lower angles of incidence the pressures on model 7 are consistently slightly less than those on model 6.

(ii) Except at zero incidence, the pressure coefficients obtained at $M = 6.85$ are on average about 5% higher than those for $M = 8.60$; this is in agreement with inviscid two-dimensional theory. For zero incidence, when the local incidence of the body facets was 10 degrees, the reason for no apparent difference between the distributions at the two Mach numbers is probably the greater boundary-layer-displacement effect at the higher Mach number.

(iii) The pressures on the body facets were not uniform, although the local incidence was constant over each facet; a similar result has been obtained at supersonic Mach numbers¹¹. However, one would not expect the pressure distribution on these facets to be uniform, unless plane shock waves were obtained. That this was not achieved was shown by shadow pictures, and a drawing showing the shape of the shock wave in cross-section inferred from shadow pictures is given in Fig.13. (From a cross-flow point of view, an attached shock wave is theoretically impossible; for a wedge semi-angle of 45 degrees, a cross-flow Mach number of about 15 or more is necessary for shock attachment¹².)

(iv) In the plane of symmetry of these bodies the shock wave lies very close to the lower ridge, the plot in Fig.13 showing that the shock approached to within 0.5 degrees of the ridge at the higher angles of incidence. This suggests that the pressure on this ridge might not be much different from that on a swept stagnation line, where the shock would be parallel to the stagnation line. So, the pressures on the ridge of model 7, plotted in Fig.14, have been compared with the pressures that would be obtained on a stagnation line at the same local incidence, i.e. $C_p = C_{p_{max}} \sin^2\theta$, where

$C_{p_{max}}$ is the stagnation pressure coefficient; it can be seen that quite close agreement is obtained. Tests by Squire¹³ at a Mach number of 4 on similar body shapes, but with "flatter" cross-sections, gave higher pressure coefficients on the ridge, but this was probably due to the greater stand-off angle of the shock under these conditions.

(v) A comparison of the mean pressure coefficients on the facets of model 7 with the mean pressure coefficients on the flat lower surfaces of models 1 and 2 is given in Figs.15 and 16, for Mach numbers of 6.85 and 8.60 respectively. The rather surprising result obtained is that at the higher local angles of incidence the mean pressure coefficients are greater on model 7 - the wing with the V-shaped lower surface - than on the wings with flat lower surfaces. A possible explanation of this effect, is that for the wing with the V-shaped lower surface, increase of incidence causes the flow pattern to approach that of two nearly plane shocks, nearly attached to the lower ridge - i.e. a near two-dimensional flow pattern in the cross-flow plane, while with the flat-bottomed wings increase of incidence results in increasing detachment of the shock, and a more three-dimensional flow pattern.

3.1.5 Models 8 and 9

The pressure distributions measured on these bodies at a Mach number of 8.60 (i.e. $\beta s/\ell = 2.14$) are plotted in Fig.17; also shown, is the effect on the half-cone body (model 8) of thin flat plate delta wings, of aspect ratios 1.5 and 2, on its upper surface (i.e. $\beta s/\ell = 3.21$ and 4.28).

The results for the cone (model 9) have been taken from Ref.14, and detailed conclusions on the pressure distributions on cones at incidence are given in that report. The pressure distributions on the curved surface of the half-cone did not differ significantly from those on the cone, except perhaps in the region near the leading edges. The addition of a delta wing to the half-cone body resulted in an increase in pressure on the body in the region near the leading edges. Further tests are to be made on various wing/body combinations, and the results will be given in a future report.

3.2 Upper surface pressure distributions

The tests described in this Note were made primarily to gain a further understanding of the flows on lower surfaces. However, some measurements of pressure distributions on upper surfaces were made during the course of these experiments; regrettably, these were of low accuracy due to the use of mercury manometers for all measurements. Some results for upper surfaces are presented, though, mainly to indicate the problems involved.

In Fig.18, results are given for model 1 at Mach numbers of 6.85 and 8.60. Two effects are immediately obvious:-

(i) The rate of decrease of pressure coefficient with increase of incidence is initially much greater at the lower Mach number.

(ii) Above a certain incidence, there is little change of pressure coefficient with incidence, the minimum mean pressure coefficients being about 0.005 at $M = 6.85$, and 0.020 at $M = 8.60$. (Vacuum pressure coefficients for these Mach numbers are -0.030 and -0.019, respectively.)

These effects are probably due to a boundary layer displacement phenomenon, but could also be due to the formation of a pair of coiled vortex sheets above the upper surface. The presence of such vortex sheets on an elliptic cone has been reported¹⁵ for Mach numbers as high as 10.

Clearly, further experiments are required before an analysis of upper surface flows can usefully be made.

4 CONCLUSIONS AND RECOMMENDATIONS FOR FUTURE WORK

(1) The comparison of experimental pressure distribution with values calculated from various inviscid flow theories and approximations was complicated by the influence of two factors:-

(a) The non-independence of upper and lower surface flow fields resulting from the shock waves not being attached to the leading-edges. The shock waves were not attached because of the high leading-edge sweep, and the large edge-angle in cross-section of the body shapes tested. This complication would also arise with bodies with blunted edges, but this was not investigated in the present tests.

(b) The effect of boundary layer displacement on the external flow field; this was small, but noticeable, at $M = 6.85$, but quite marked for $M = 8.60$. The values of the viscous interaction parameter M^3/R_L^2 (based on body length) were 0.2 at $M = 6.85$ and 0.65 for $M = 8.60$.

Unfortunately, the above two effects were often of the same magnitude as the maximum experimental error, so there is a need for further more detailed experimental work before these effects can be separated and more accurately defined. If tests of an essentially inviscid nature are required (i.e. $M^3/R_L^2 < 0.2$) to specifically check an inviscid flow theory, for example, then these could be done more conveniently in a larger, lower Mach number, facility rather than in the R.A.E. 7 in. x 7 in. intermittent hypersonic tunnel. An example of such a test, would be an experiment to check the theory of Babaev⁹ for the flat plate delta wing at incidence.

(2) In general, the estimation of pressure distributions by simple empirical methods which assume that pressure is dependent on the local incidence of the body surface to the free stream left certain discrepancies to be explored further. For example, it was found that pressure distributions on bodies with flat surfaces were generally not uniform. For a body shape

composed of two flat triangular lower surfaces, designed so as to support a plane attached shock wave at chosen conditions of Mach number and incidence, a uniform pressure distribution was obtained, however. There is a need for experiments on body shapes with flat surfaces under conditions where the shock is attached to the leading edges, where complications arising from the non-independence of upper and lower surface flows do not arise.

(3) As regards overall forces, the tangent-wedge approximation gave reasonable estimates for body shapes with flat surfaces, for the lower angles of incidence. The Newtonian and tangent-cone approximations always gave underestimates in the range of angles of incidence covered ($\alpha \leq 29^\circ$).

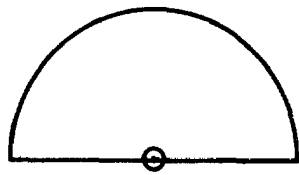
(4) From the few measurements made of upper surface pressure distributions, it was clear that there were quite large differences in behaviour between Mach numbers of 6.85 and 8.60. These differences are probably due to boundary-layer-displacement effects, and possibly flow separation phenomena. Further experiments are needed before an analysis of upper surface flows can be usefully made.

REFERENCES

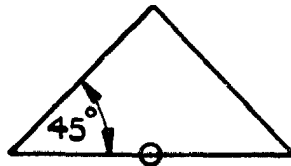
- | <u>No.</u> | <u>Author</u> | <u>Title, etc.</u> |
|------------|-----------------------------------|---|
| 1 | Peckham, D.H. | A proposed programme of wind tunnel tests at hypersonic speeds to investigate the lifting properties of geometrically slender shapes.
R.A.E. Tech. Note No. Aero 2730.
A.R.C. 22594. December 1960. |
| 2 | Peckham, D.H. | On three-dimensional bodies of delta planform which can support plane attached shock waves.
A.R.C. C.P. 640. March 1962 |
| 3 | Crabtree, L.F. | Survey of inviscid hypersonic flow theory for geometrically slender shapes.
R.A.E. Tech. Note No. Aero 2695. June 1960. |
| 4 | Squire, L.C. | Pressure distributions flow patterns at $M = 4.0$ on some delta wings.
Part II 'Flat' wings.
A.R.C. R & M 3373. February 1963 |
| 5 | Bertram, M.H.
Blackstock, T.A. | Some simple solutions to the problem of predicting boundary layer self-induced pressures.
NASA TN D-798. April 1961. |
| 6 | Hayes, W.D.
Probstein, R.F. | Hypersonic flow theory.
Academic Press, 1959. p.345. |

REFERENCES (CONTD)

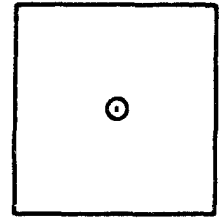
<u>No.</u>	<u>Author</u>	<u>Title, etc.</u>
7	Treadgold, D.A.	Private communication.
8	Bagley, J.A.	An estimate of the lateral forces and moments on yawed caret wings. R.A.E. Tech. Note No. Aero 2813. A.R.C. 24057. April 1962.
9	Babaev, D.A.	Supersonic flow past the lower surface of a delta wing. AIAA Journal Vol.1 No.9. September 1963.
10	Goebel, T.P. Martin, J.J. Boyd, J.A.	Factors affecting lift-drag ratios at Mach numbers from 5 to 20. AIAA Journal Vol.1 No.3. March 1963.
11	Akers, A.	Some studies of pressure distributions on the windward surfaces of conical bodies at high supersonic speeds. A.R.C. C.P. 723. September 1963.
12	Ames Research Staff	Equations, tables and charts for compressible flow. NACA Report 1135.
13	Squire, L.C.	Pressure distributions and flow patterns on some conical shapes with sharp edges and symmetrical cross-sections at $M = 4$. A.R.C. R & M 3340. June 1962
14	Peckham, D.H.	Experiments at hypersonic speeds on circular cones at incidence. A.R.C. C.P. 702. January 1963
15	Palko, R.L. Ray, A.D.	Pressure distribution and flow visualisation tests of a 1.5 elliptic cone at Mach 10. AEDC-TDR-63-163.
16	Gatherall, D.	Boundary layer characteristics of caret wings. A.R.C. C.P. 694. May 1963



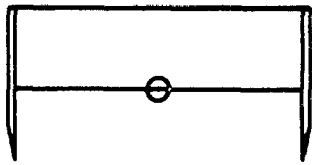
1



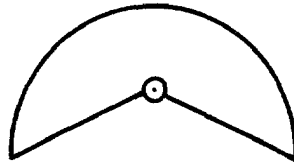
2



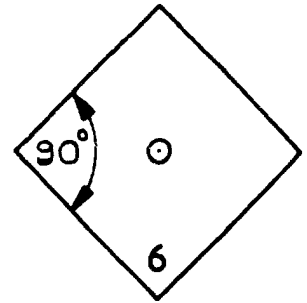
3



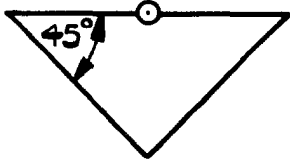
4



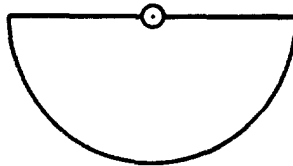
5



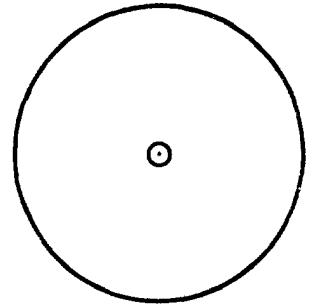
6



7

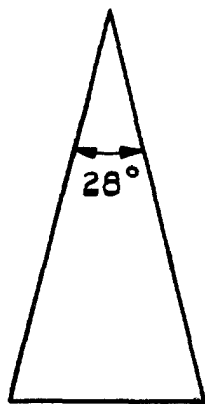


8

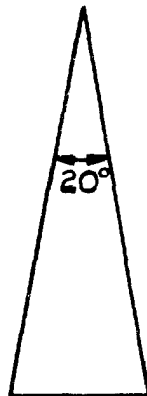


9

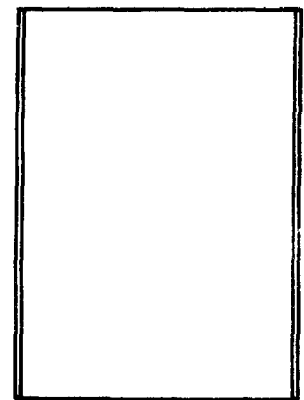
DETAILS OF CROSS-SECTIONS



MODELS 1,2,5,6,7,8,9
ASPECT RATIO 1



MODEL 3
ASPECT RATIO 0.707



MODEL 4

DETAILS OF PLANFORMS

⊙ REFERENCE AXIS FOR MODEL INCIDENCE α

FIG. 1. GEOMETRY OF MODELS.

I ESTIMATED MAX. EXPTL. ERROR

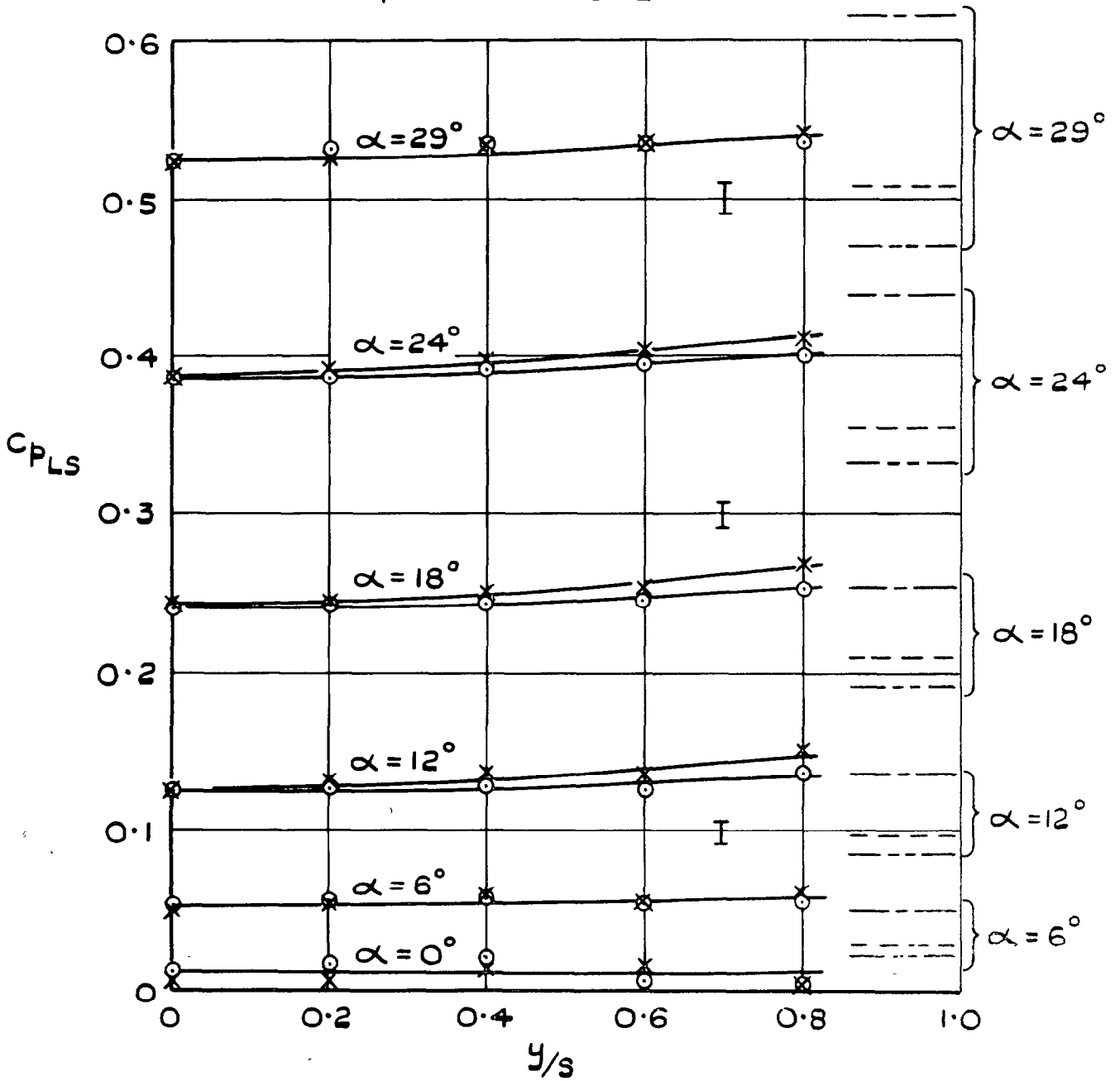
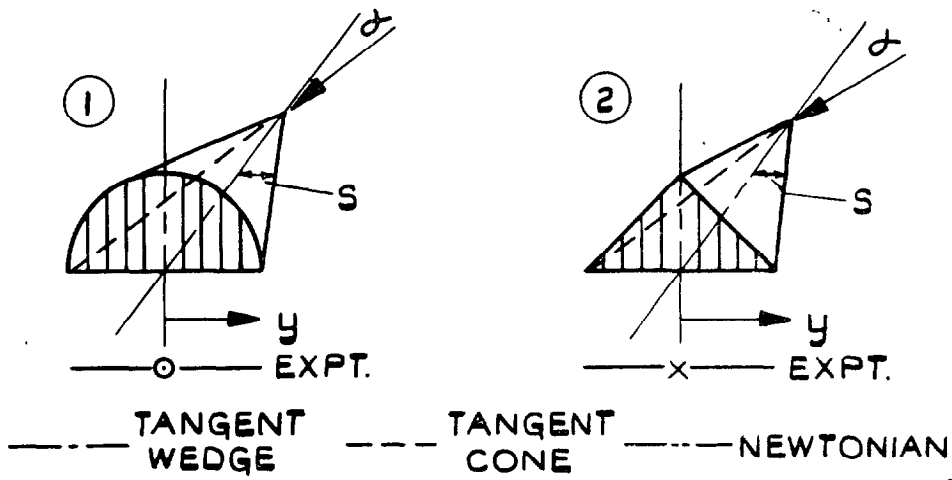


FIG. 2. LOWER SURFACE PRESSURE DISTRIBUTIONS FOR MODELS 1 AND 2. $M=6.85$ $\beta S/l=1.7$.

I ESTIMATED MAX. EXPTL. ERROR

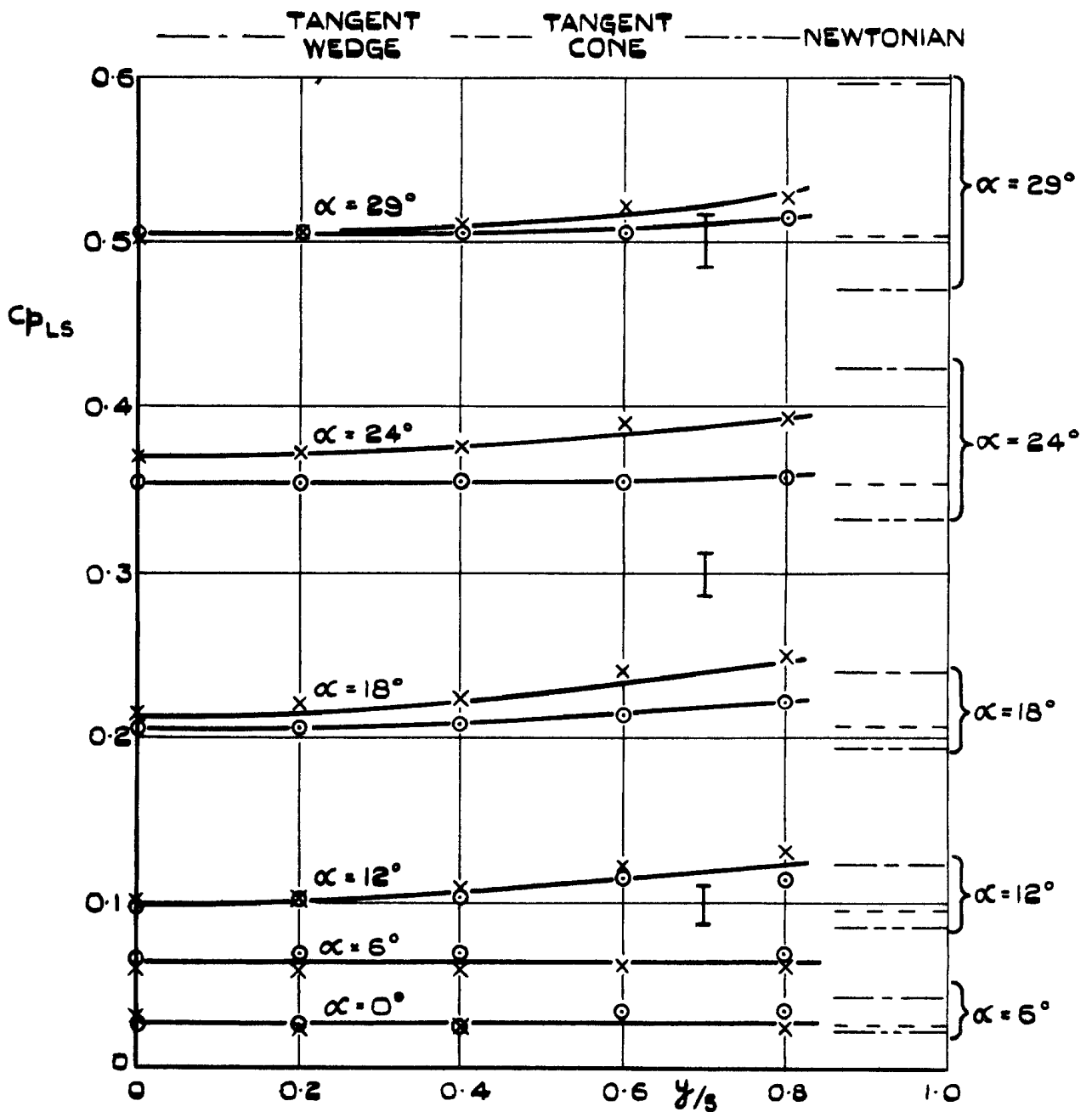
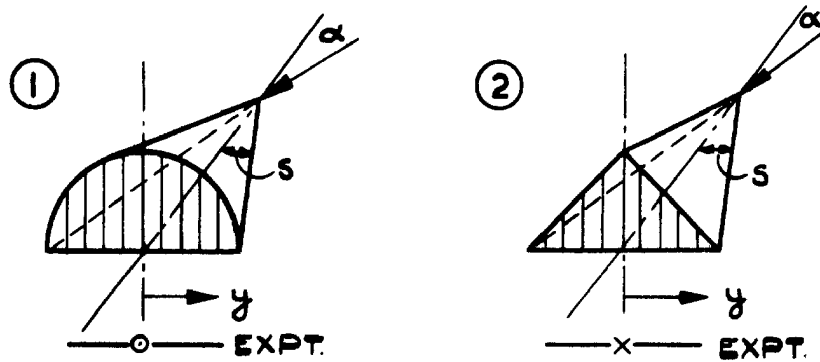


FIG.3. LOWER SURFACE PRESSURE DISTRIBUTIONS FOR MODELS 1 AND 2 $M=8.60$ $\beta s/b = 2.14$

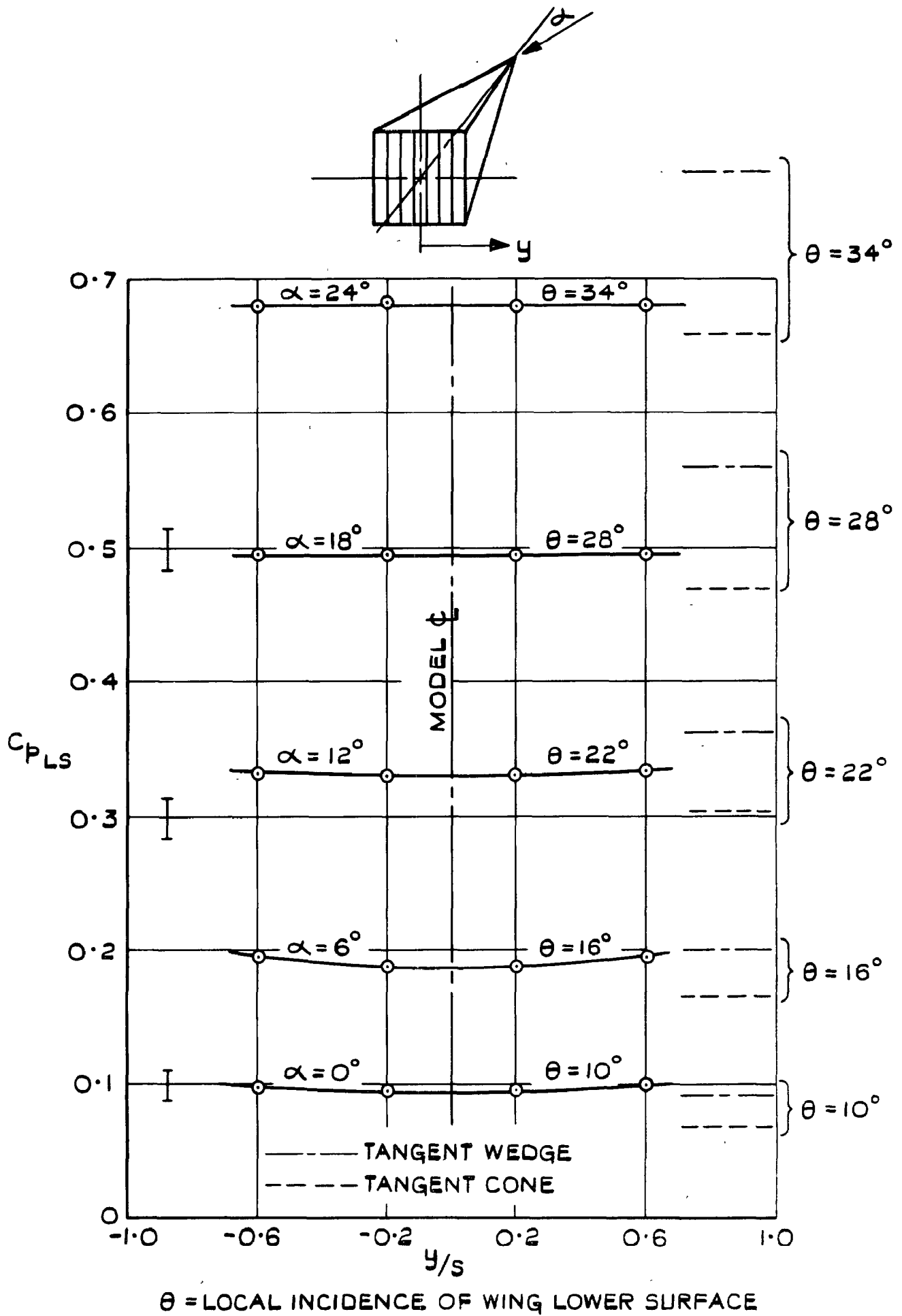


FIG. 4. LOWER SURFACE PRESSURE DISTRIBUTIONS FOR MODEL 3, $M=8.60$.

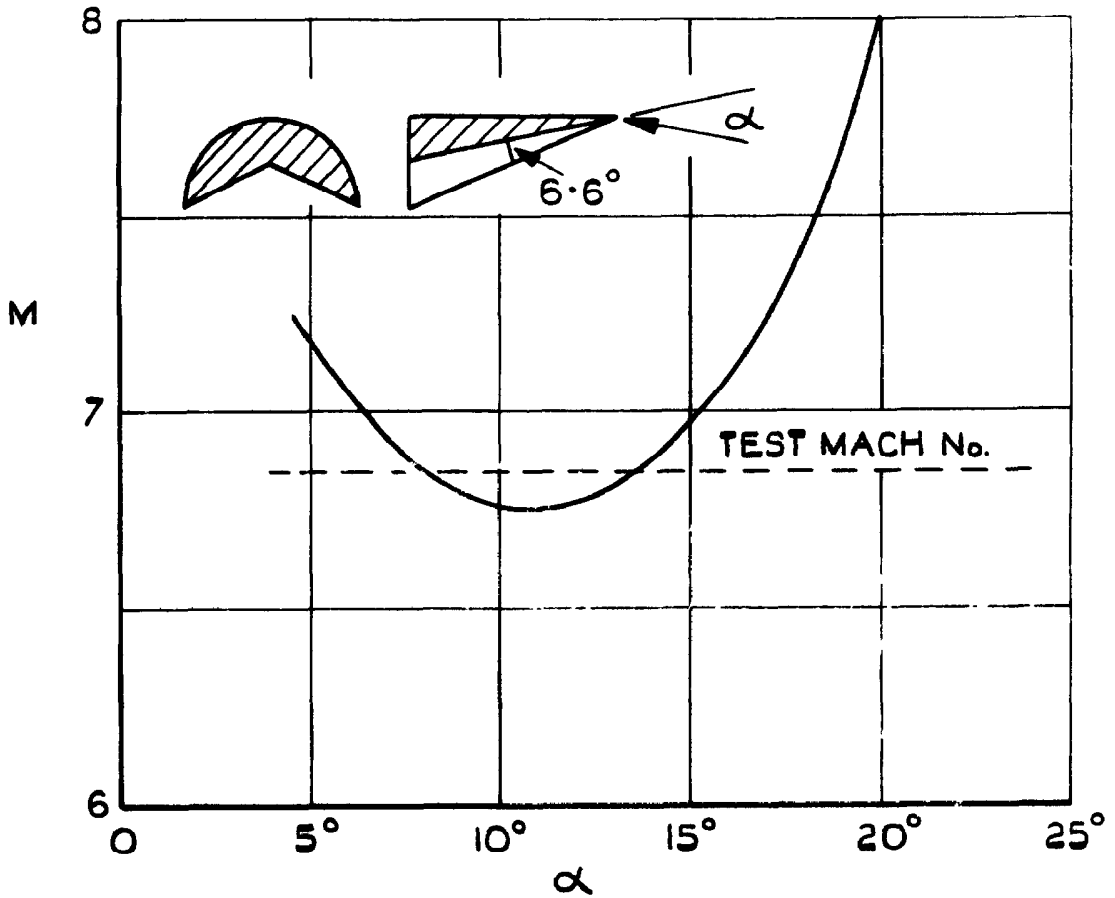


FIG. 5. MACH NUMBER TO GIVE ATTACHED PLANE SHOCK WAVE ON WINGS 4 AND 5 (THEORETICAL)

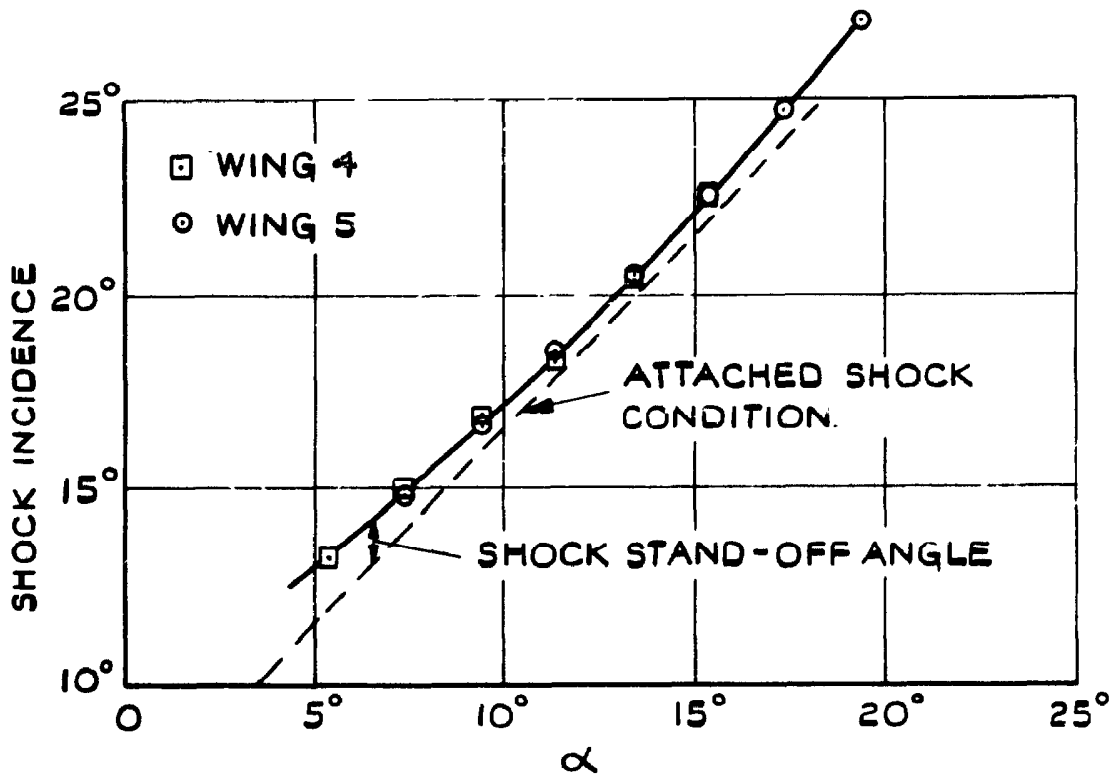
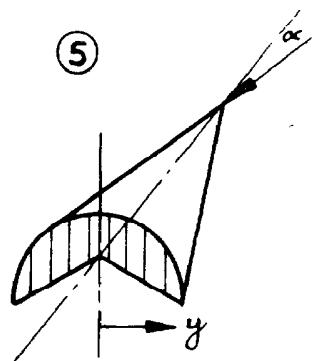
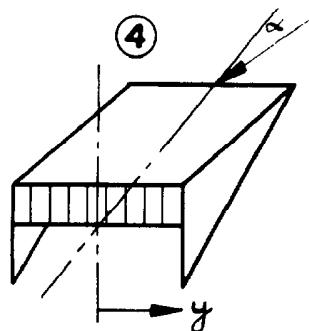


FIG. 6. VARIATION OF SHOCK STAND-OFF ANGLE WITH INCIDENCE ON WINGS 4 AND 5. EXPERIMENT AT $M=6.85$



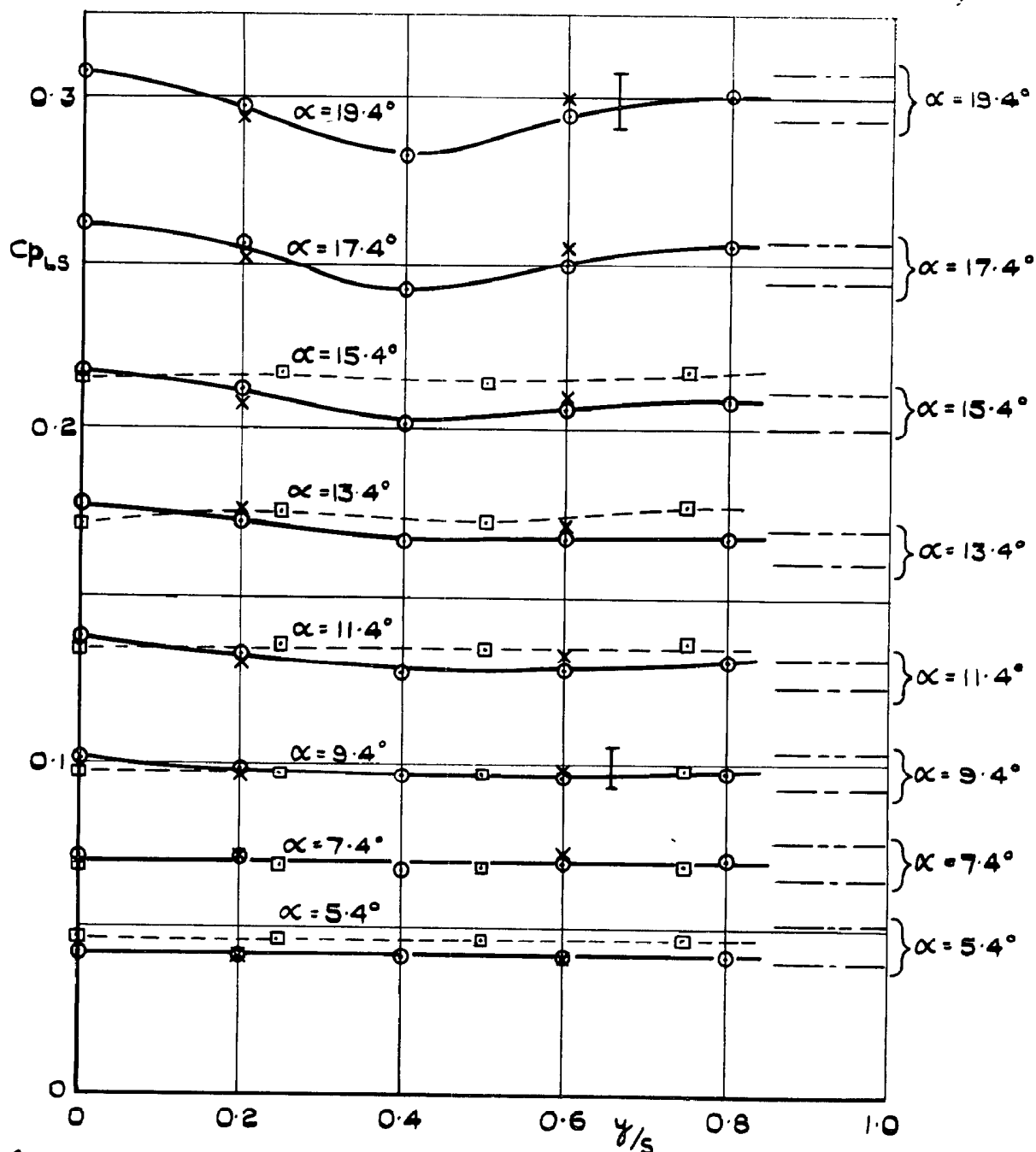
---□---

—○— γ/s +ve

—x— γ/s -ve

----- TANGENT WEDGE

$$C_p = \frac{5}{3} \left(\sin^2 \zeta - \frac{1}{M^2} \right)$$



ζ = MEASURED SHOCK ANGLE

FIG.7. LOWER SURFACE PRESSURE DISTRIBUTIONS FOR WINGS 4 AND 5 $M=6.85$

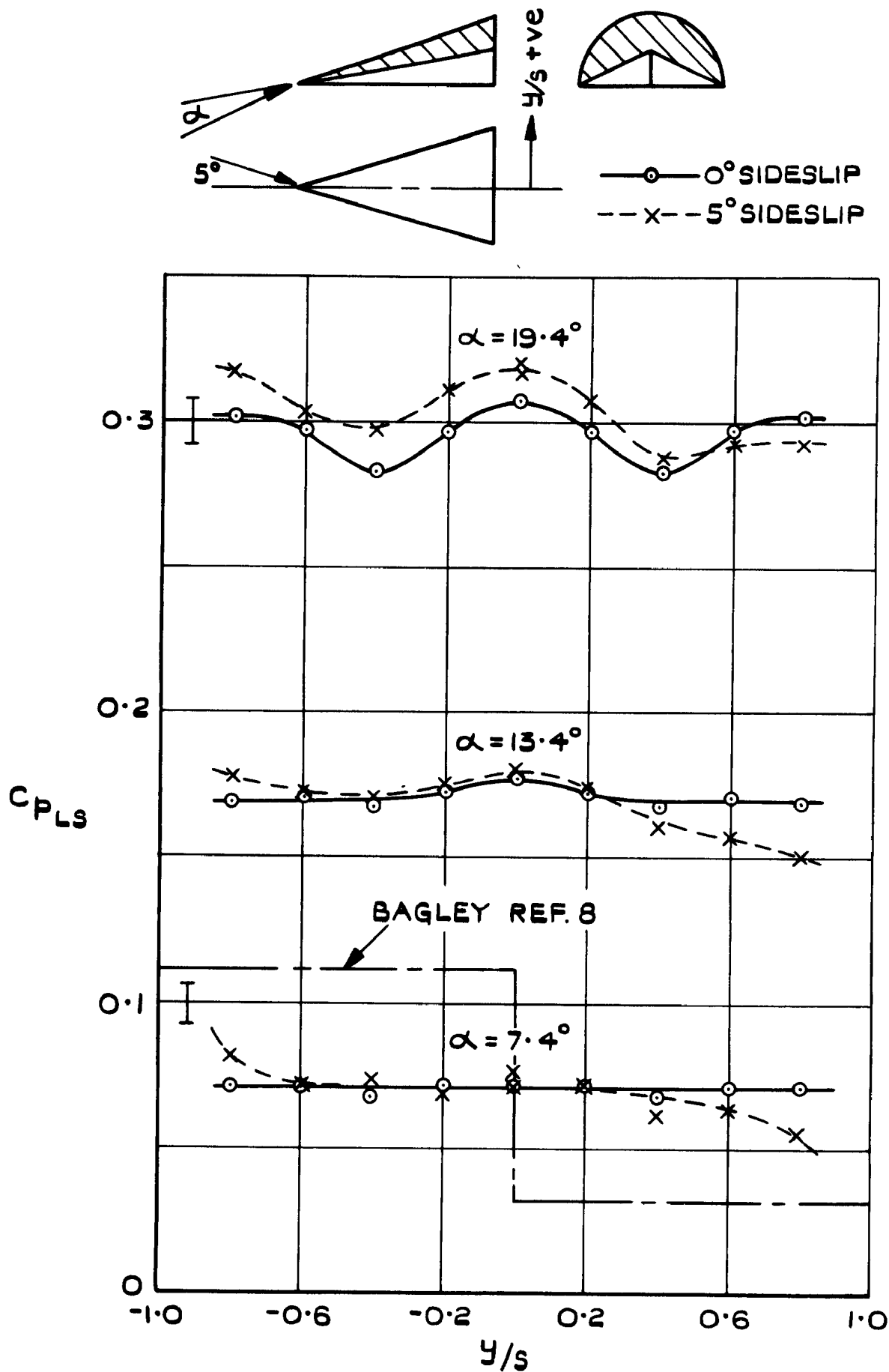


FIG. 8. EFFECT OF POSITIVE SIDESLIP ON LOWER SURFACE PRESSURES ON WING 5. $M=6.85$

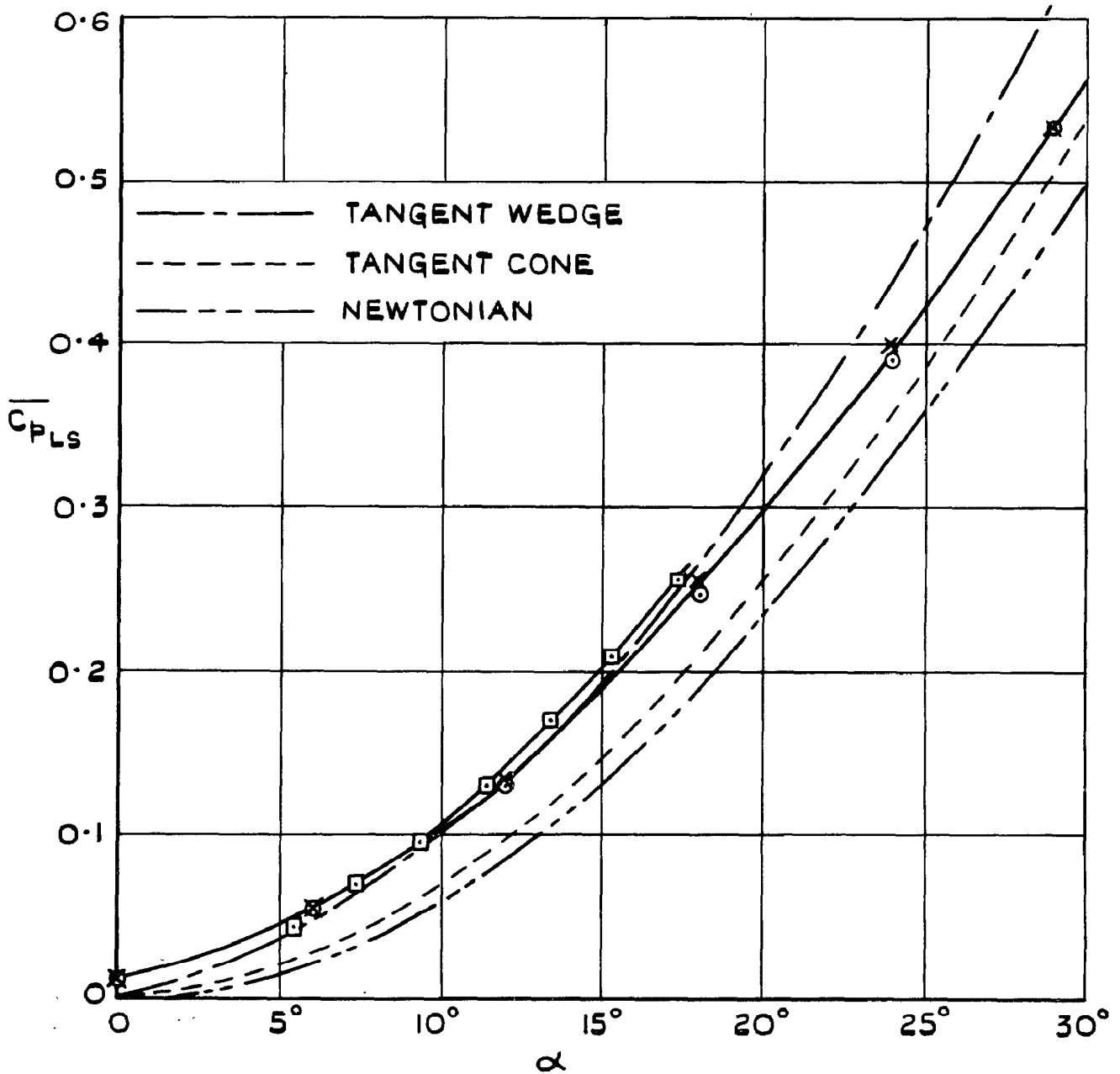
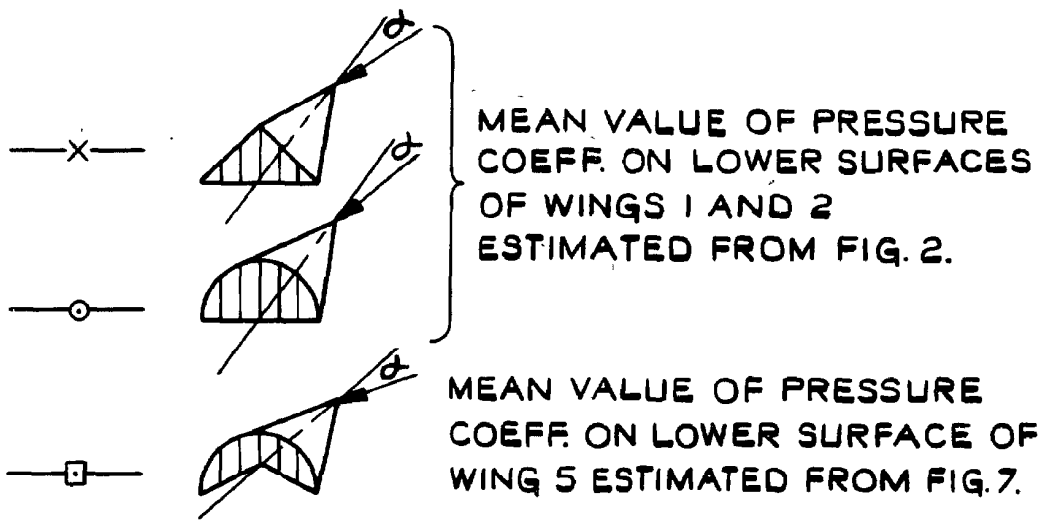
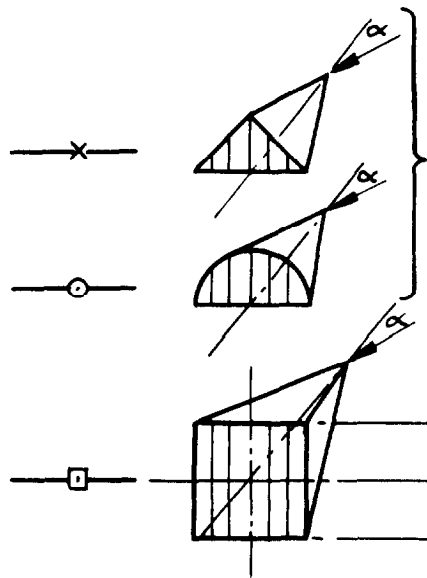


FIG. 9. VARIATION WITH INCIDENCE OF MEAN PRESSURE COEFFICIENT ON LOWER SURFACES OF WINGS 1, 2 AND 5. $M=6.85$



MEAN VALUE OF PRESSURE COEFF. ON LOWER SURFACES OF WINGS 1 AND 2 ESTIMATED FROM FIG. 3

MEAN VALUE OF PRESSURE COEFF. ON LOWER SURFACE OF WING 3 ESTIMATED FROM FIG. 4

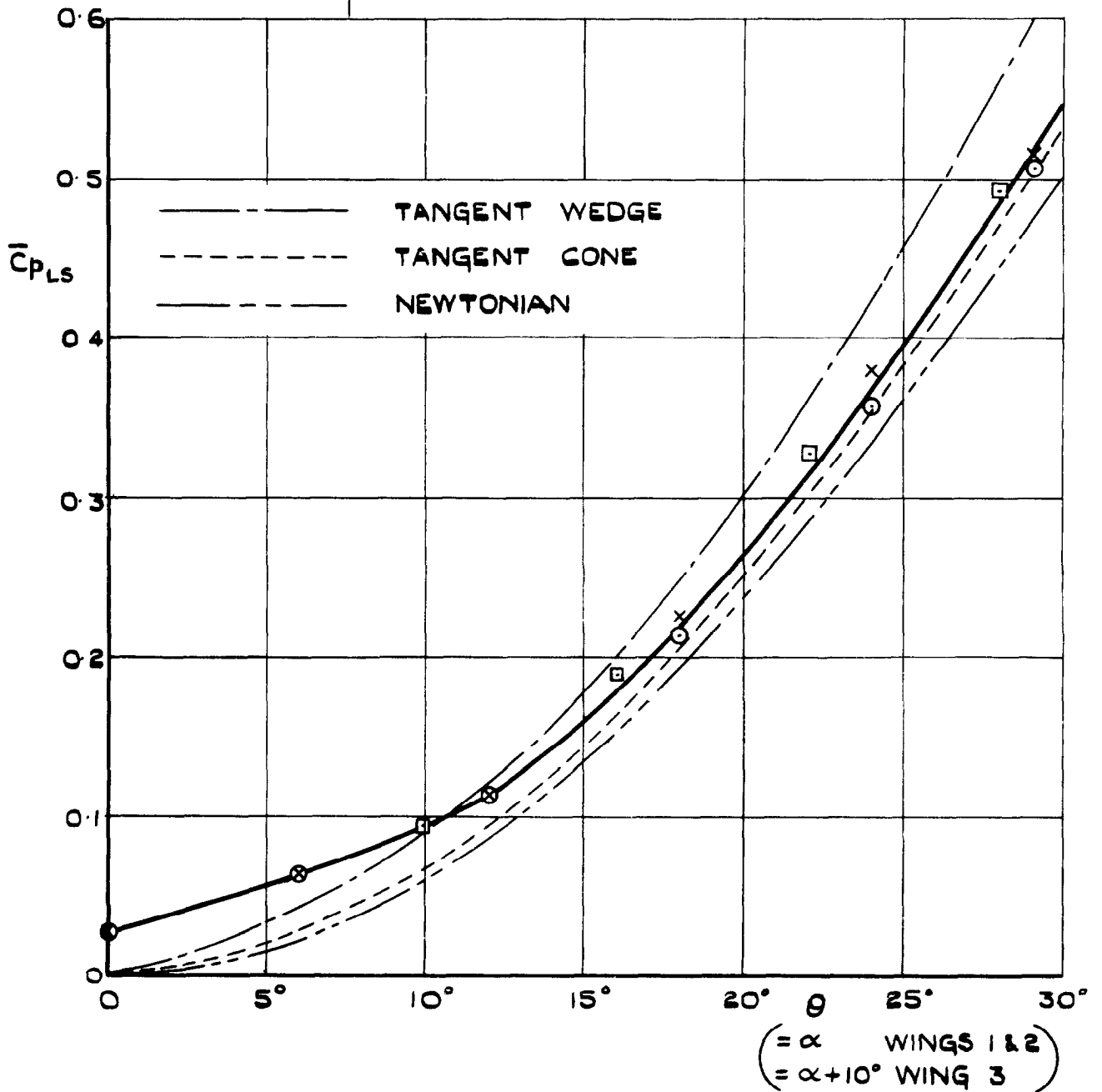
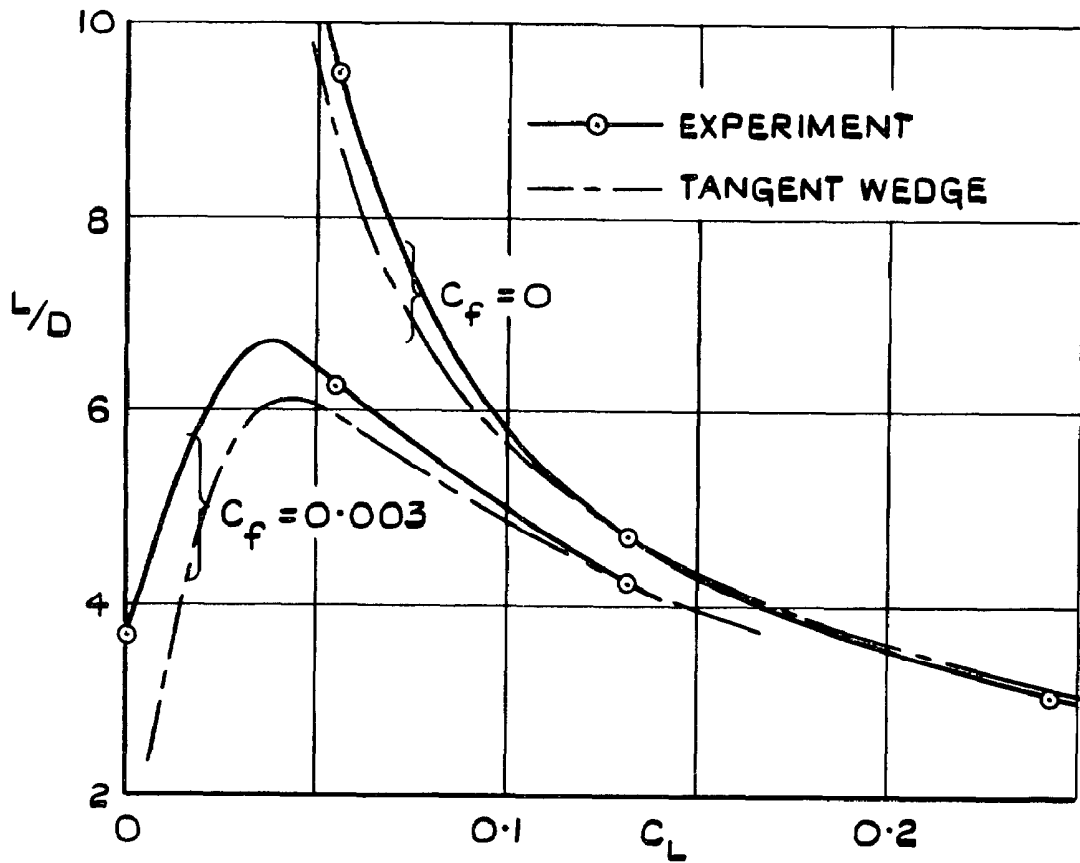
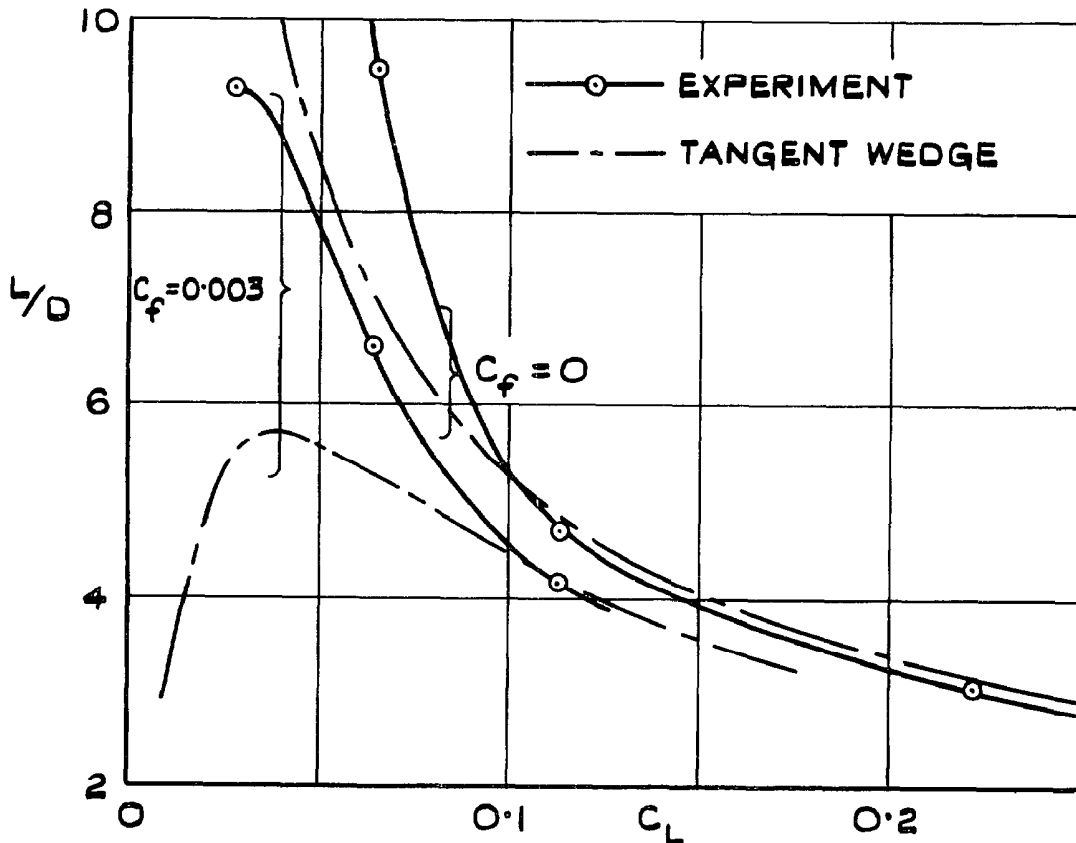


FIG. 10. VARIATION WITH INCIDENCE OF MEAN PRESSURE COEFFICIENT ON LOWER SURFACES OF WINGS 1, 2 AND 3. $M=8.60$



(a) $M = 6.85 \quad M^3/\sqrt{R_L} = 0.20$



(b) $M = 8.60 \quad M^3/\sqrt{R_L} = 0.65$

FIG. II. (a & b) EFFECT OF VISCOUS INTERACTION ON LIFT/DRA RATIO OBTAINED FROM LOWER SURFACES OF WINGS 1 & 2.

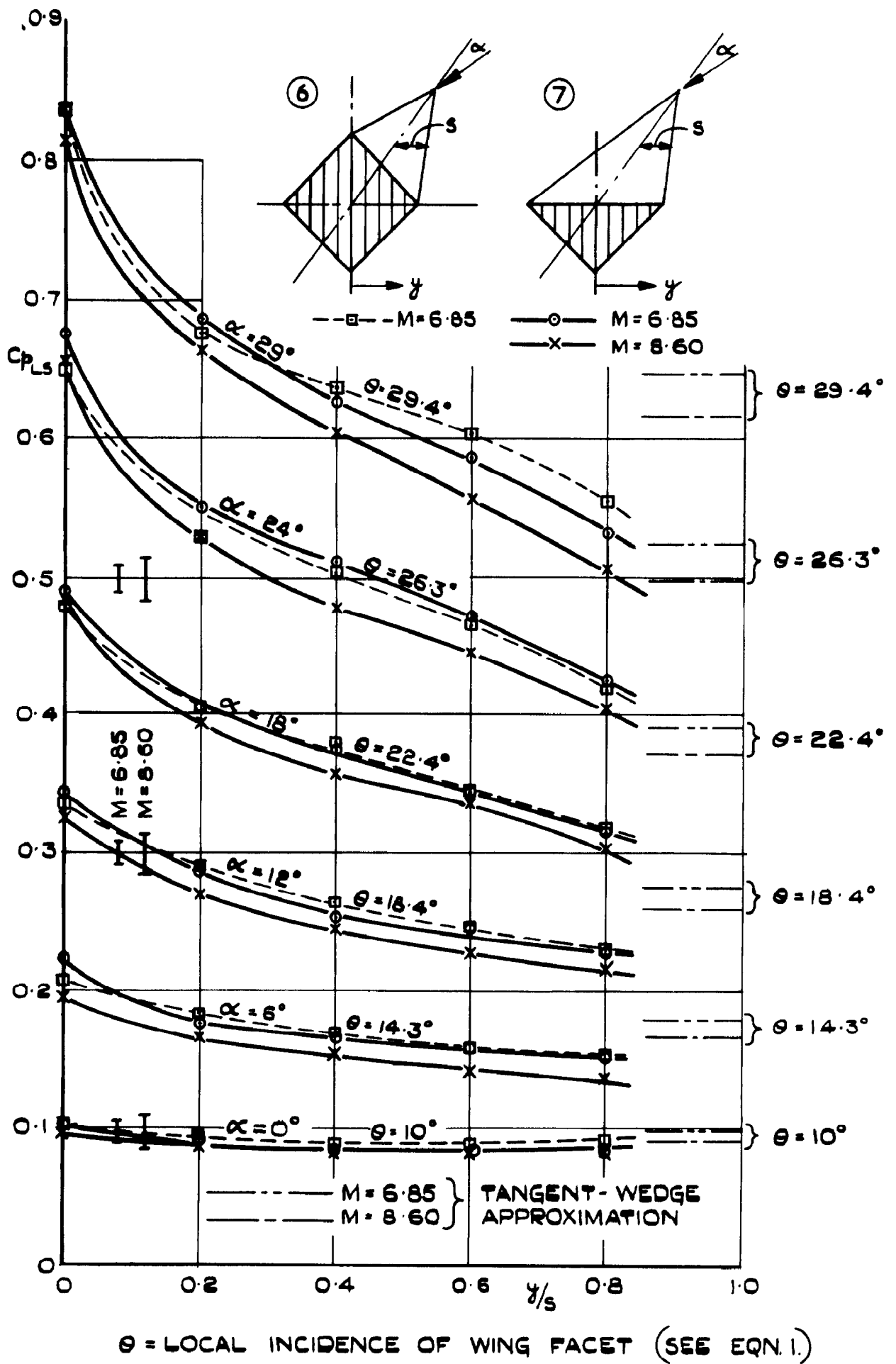
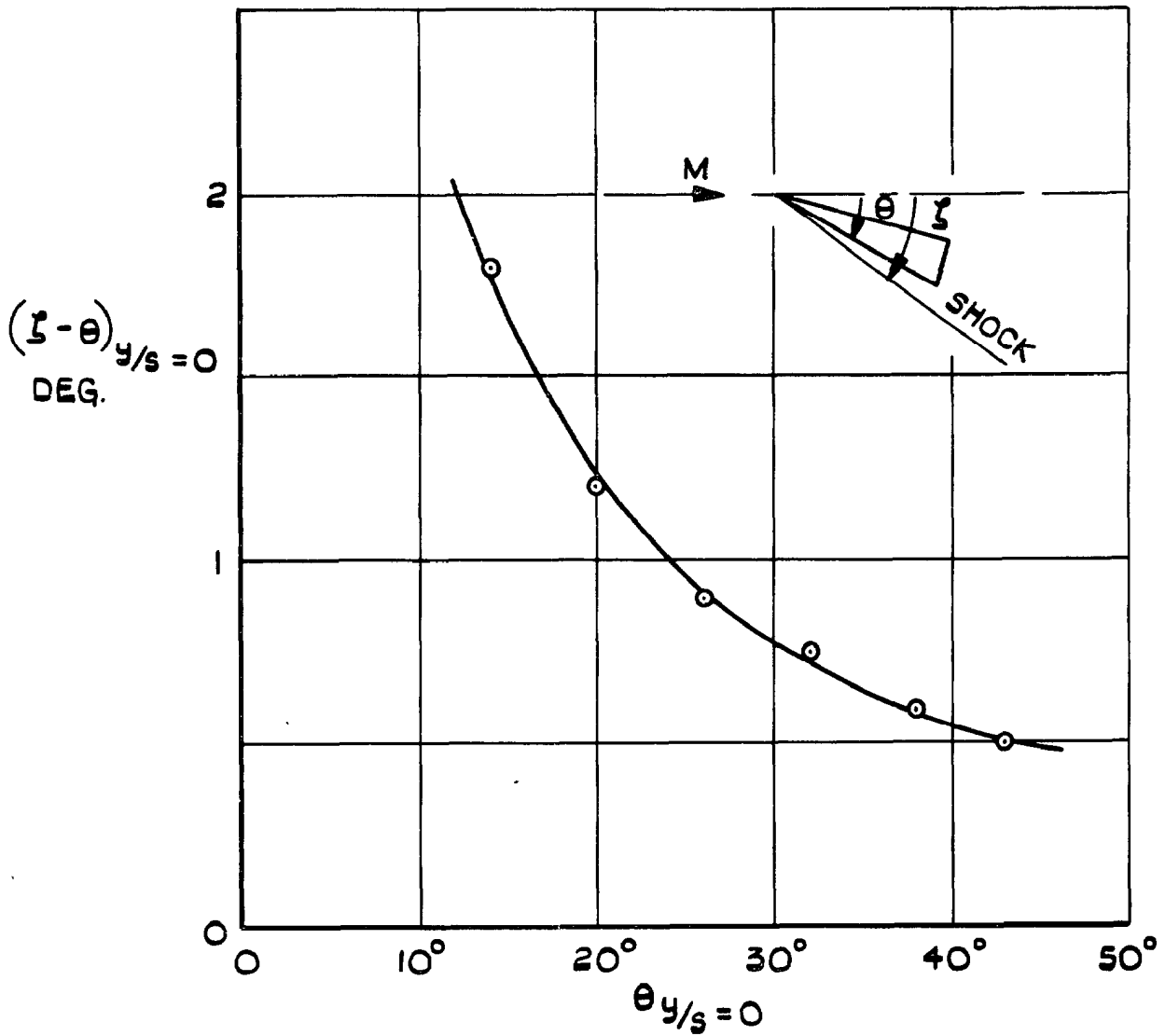
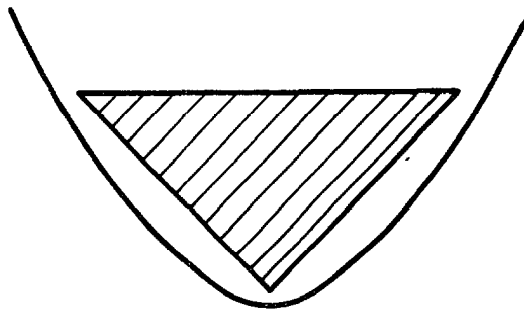


FIG. 12. PRESSURE DISTRIBUTIONS OVER THE LOWER SURFACES OF WINGS 6 AND 7 AT $M = 6.85$ AND 8.60

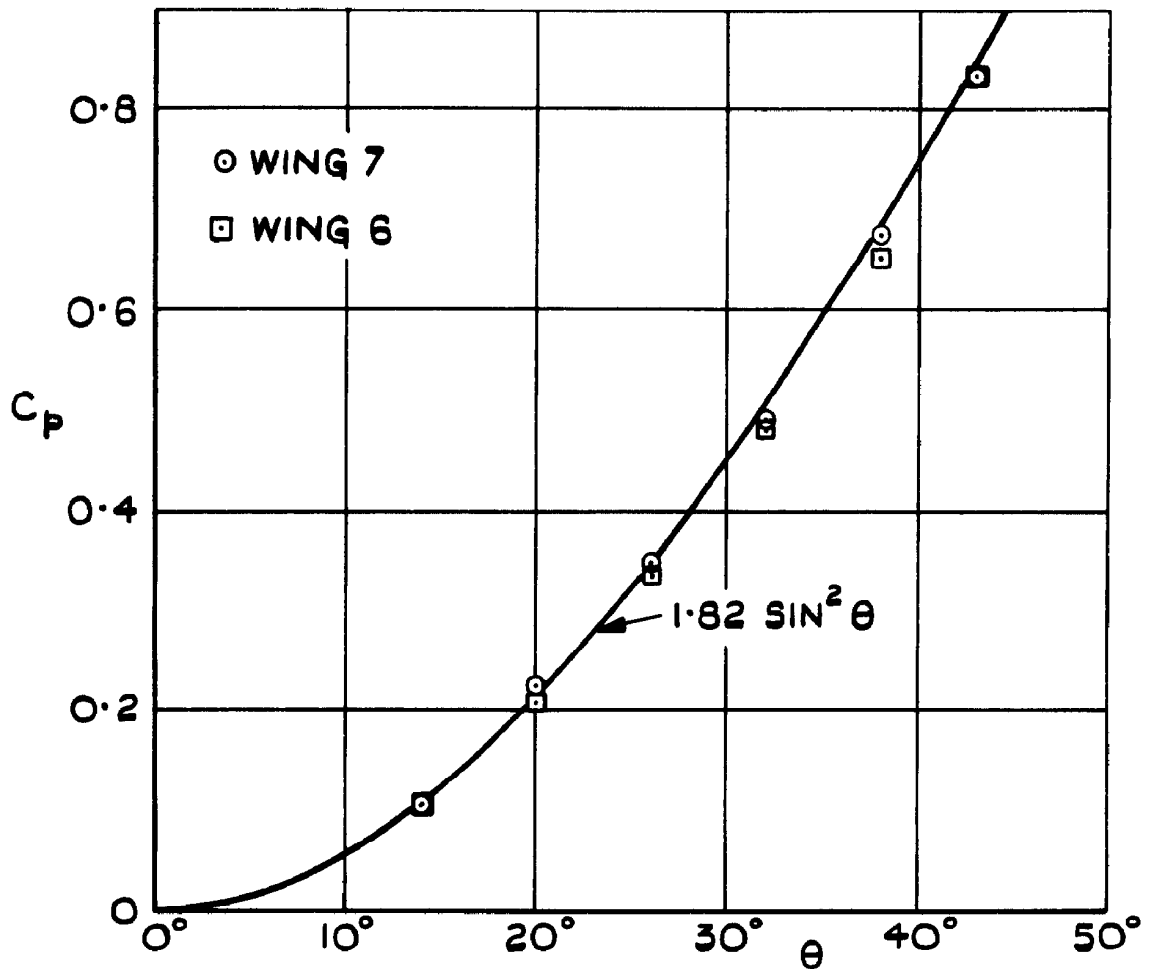


(a) SHOCK STAND-OFF ANGLE

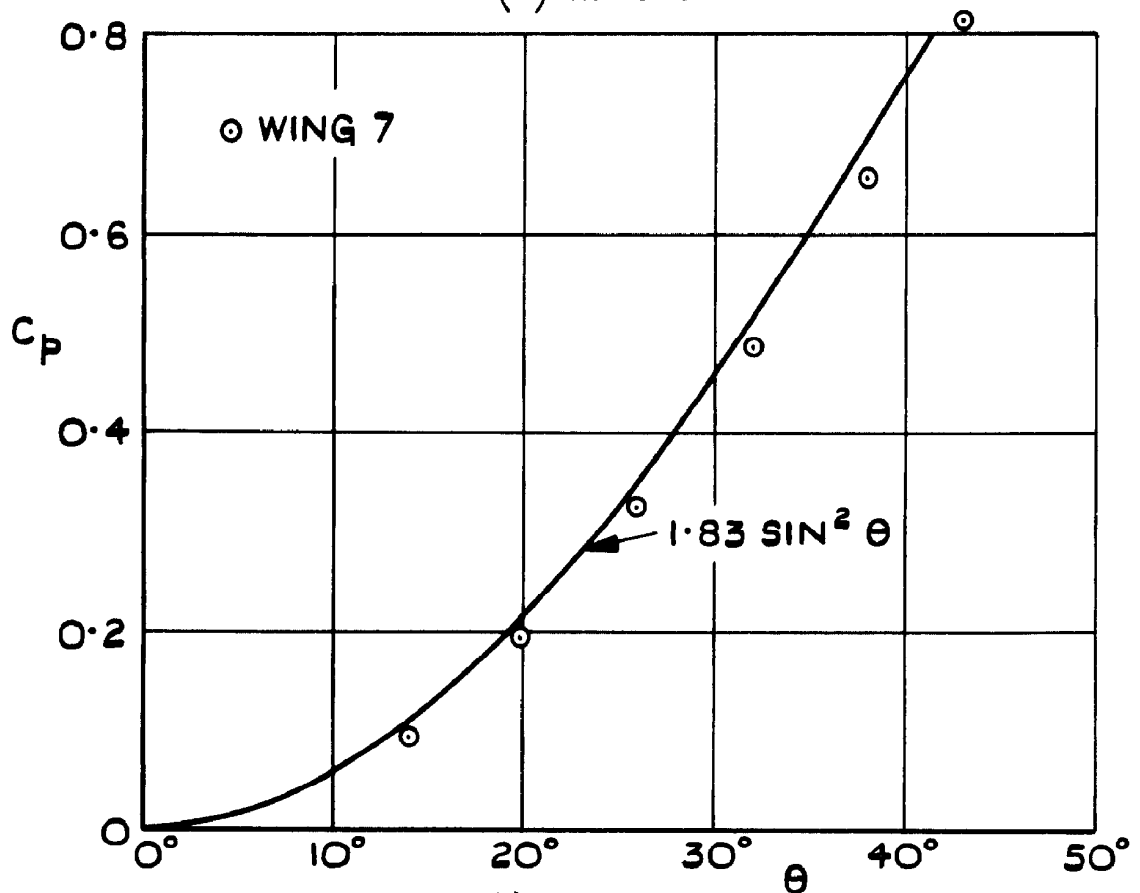


(b) SHOCK SHAPE IN CROSS-SECTION INFERRED FROM SHADOW PHOTOGRAPHS

FIG. 13. (a & b) GEOMETRY OF SHOCK WAVE ON MODEL 7. $M = 6.85$



(a) $M = 6.85$



(b) $M = 8.60$

$\theta = \text{INCIDENCE OF LOWER RIDGE LINE} = \alpha + 14^\circ$

FIG. 14. (a & b) LOWER RIDGE-LINE PRESSURES ON WINGS 6 AND 7.

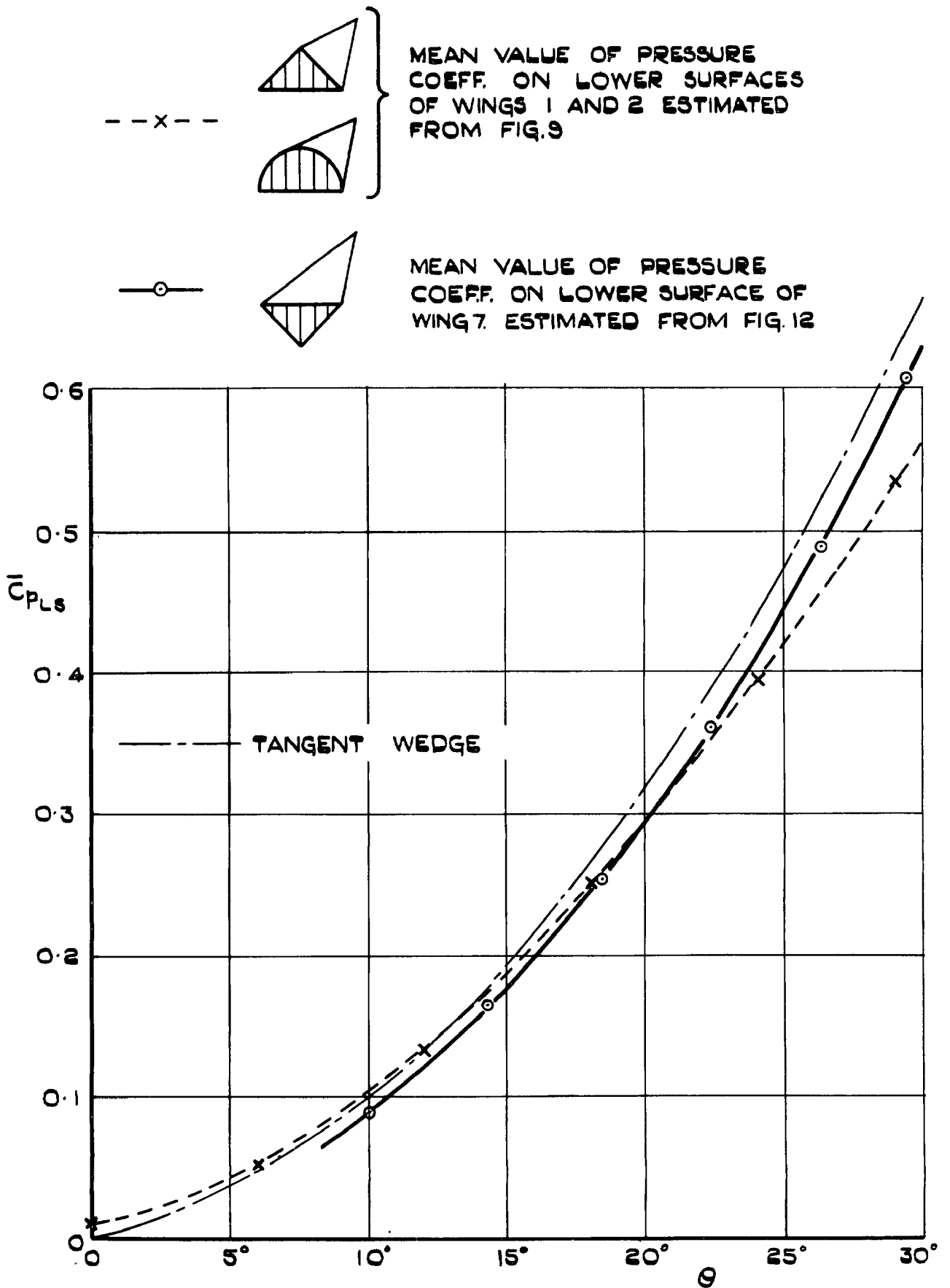


FIG.15. VARIATION WITH LOCAL INCIDENCE OF MEAN PRESSURE COEFFICIENT ON LOWER SURFACES OF WINGS 1, 2 AND 7. $M = 6.85$

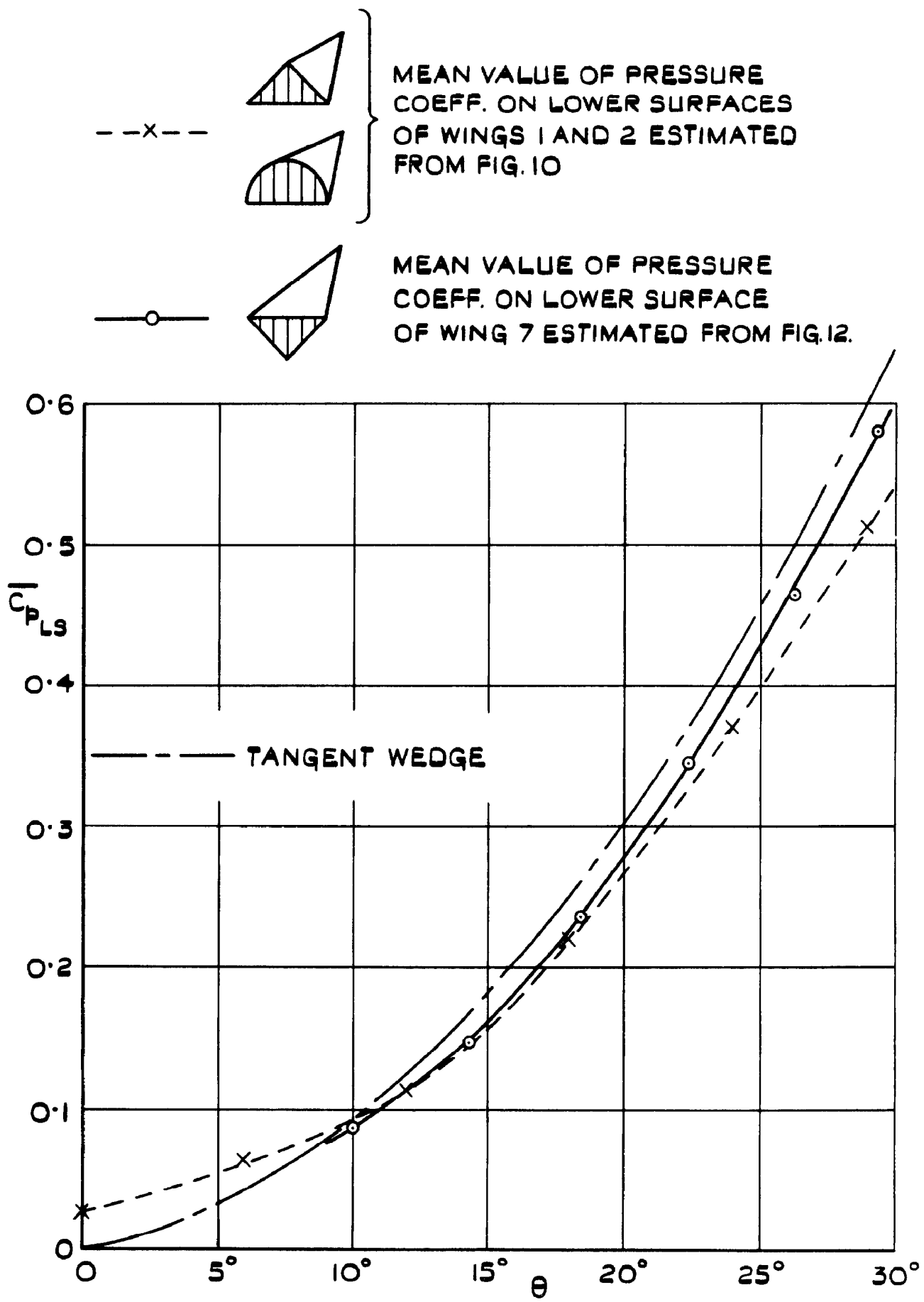


FIG. 16. VARIATION WITH LOCAL INCIDENCE OF MEAN PRESSURE COEFFICIENT ON LOWER SURFACES OF WINGS 1,2 AND 7. $M=8.60$

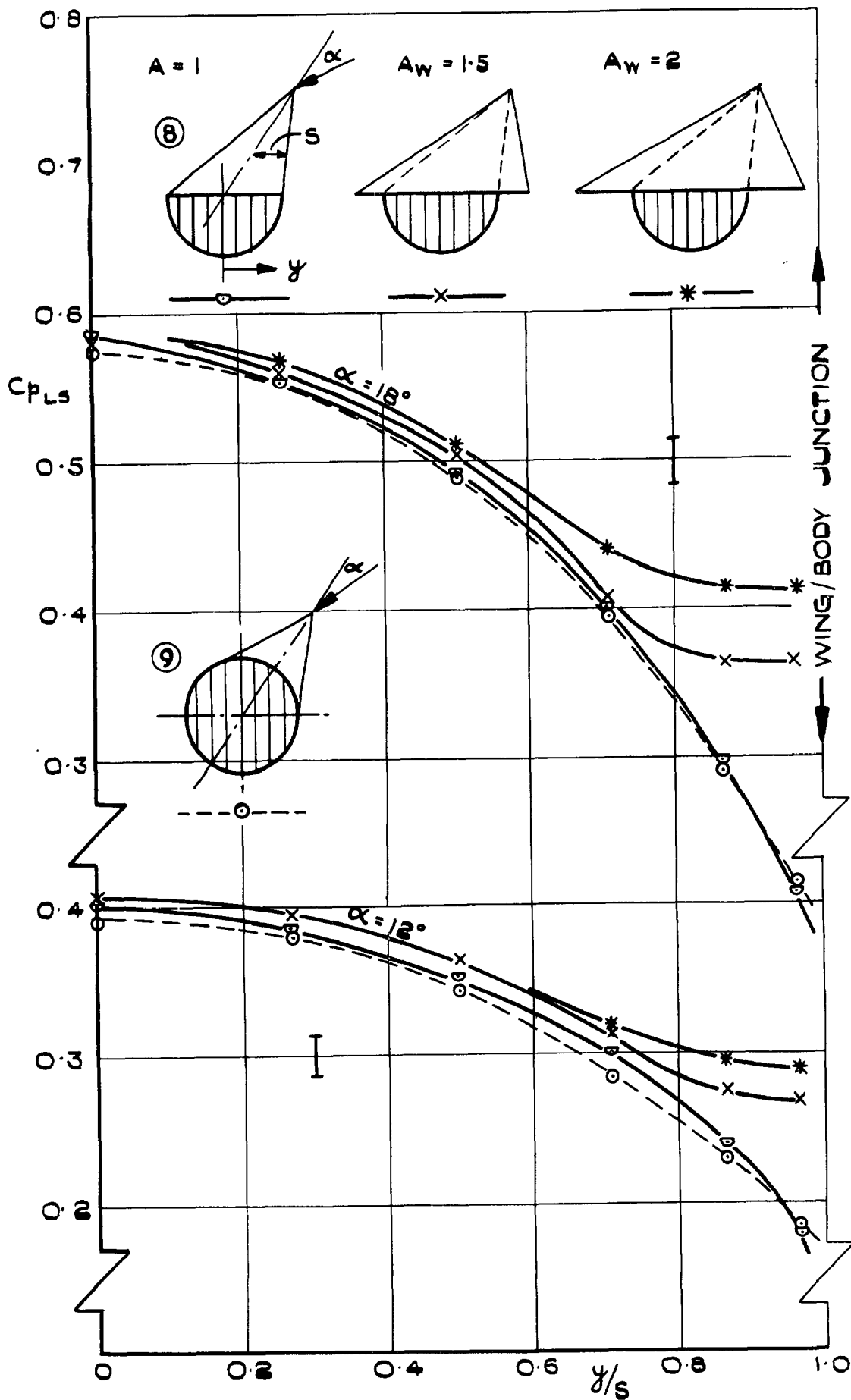


FIG. 17 LOWER SURFACE PRESSURE DISTRIBUTIONS FOR MODELS 8 AND 9, INCLUDING EFFECT OF INTERFERENCE FROM DELTA WINGS $M = 8.60$

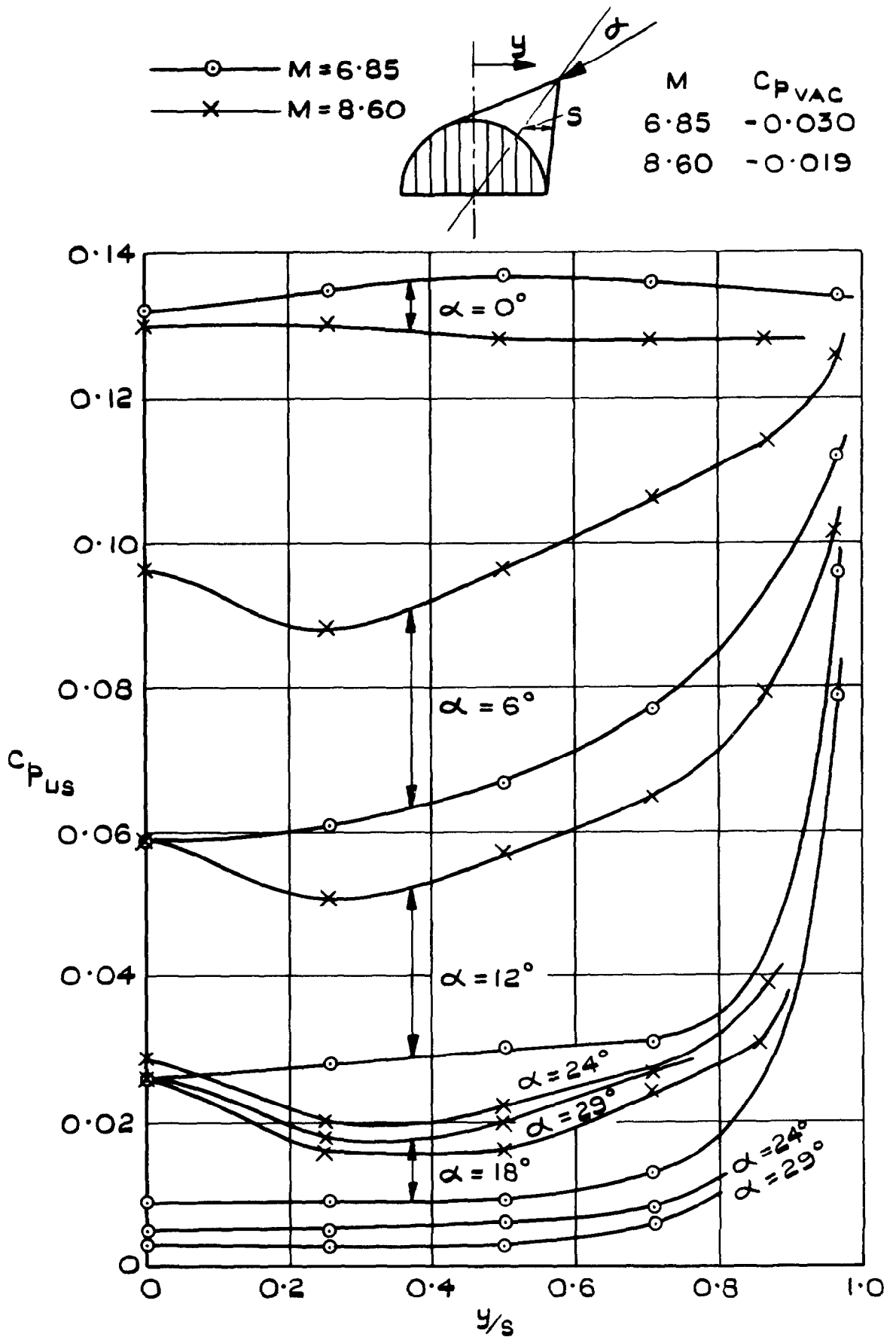


FIG. 18. UPPER SURFACE PRESSURE DISTRIBUTIONS FOR MODEL 1. M = 6.85 AND 8.60.

A.R.C. C.P. No. 791

533.696:
533.6.048.2:
533.6.011.55

PRESSURE DISTRIBUTION MEASUREMENTS ON A SERIES OF SLENDER DELTA BODY SHAPES AT MACH NUMBERS OF 6.85 AND 8.60. Peckham, D.H. February 1964.

Results are given of a wind tunnel programme made to study the pressure distributions, mainly on the windward surfaces, of a series of simple body shapes, over a range of angles of incidence up to 29 degrees. It was found that the comparison of experimental pressure distributions with values calculated from various inviscid flow theories and approximations, was complicated by the non-independence of upper and lower surface flow fields, and by boundary-layer-displacement effects. From the few measurements made of upper surface pressure distributions, quite large differences in behaviour were observed between Mach numbers of 6.85 and 8.60. Recommendations are made in regard to future experiments.

A.R.C. C.P. No. 791

533.696:
533.6.048.2:
533.6.011.55

PRESSURE DISTRIBUTION MEASUREMENTS ON A SERIES OF SLENDER DELTA BODY SHAPES AT MACH NUMBERS OF 6.85 AND 8.60. Peckham, D.H. February 1964.

Results are given of a wind tunnel programme made to study the pressure distributions, mainly on the windward surfaces, of a series of simple body shapes, over a range of angles of incidence up to 29 degrees. It was found that the comparison of experimental pressure distributions with values calculated from various inviscid flow theories and approximations, was complicated by the non-independence of upper and lower surface flow fields, and by boundary-layer-displacement effects. From the few measurements made of upper surface pressure distributions, quite large differences in behaviour were observed between Mach numbers of 6.85 and 8.60. Recommendations are made in regard to future experiments.

© *Crown Copyright 1965*

Published by
HER MAJESTY'S STATIONERY OFFICE

To be purchased from
York House, Kingsway, London W.C.2
423 Oxford Street, London W.1
13A Castle Street, Edinburgh 2
109 St. Mary Street, Cardiff
39 King Street, Manchester 2
50 Fairfax Street, Bristol 1
35 Smallbrook, Ringway, Birmingham 5
80 Chichester Street, Belfast 1
or through any bookseller